Title

The common *TMEM173 HAQ, AQ* alleles rescue CD4 T cellpenia, restore T-regs, and prevent *SAVI (N153S)* inflammatory disease in mice.

Short Title

TMEM173 HAQ, AQ alleles prevent SAVI disease.

Authors

Alexandra Aybar-Torres,[1] Lennon A Saldarriaga,[1] Ann T. Pham,[1] Amir M. Emtiazjoo,[1] Ashish K Sharma,[2] Andrew J. Bryant,[1] Lei Jin[1*]

Affiliations

[1]Division of Pulmonary, Critical Care and Sleep Medicine, Department of Medicine, University of Florida, Gainesville, FL 32610, U.S.A.

[2]Division of Vascular Surgery & Endovascular Therapy, Department of Surgery, University of Florida, Gainesville, FL 32610, U.S.A.

[*]Corresponding Author: Lei Jin, Ph.D. Email: lei.jin@medicine.ufl.edu

Abstract

The significance of STING (encoded by the *TMEM173* gene), in tissue inflammation and cancer immunotherapy has been increasingly recognized. Intriguingly, common human *STING* alleles R71H-G230A-R293Q (*HAQ)* and G230A-R293Q (*AQ*) are carried by ~60% of East Asians and ~40% of Africans, respectively. Here, we examine the modulatory effects of *HAQ, AQ* alleles on STING-associated vasculopathy with onset in infancy (SAVI), an autosomal dominant, fatal inflammatory disease caused by gain-of-function human *STING* mutations. CD4 T cellpenia is evident in SAVI patients and mouse models. Using STING knock-in mice expressing common human *STING* alleles *HAQ*, *AQ*, and *Q293*, we found that *HAQ, AQ*, and *Q293* splenocytes resist STING-mediated cell death *ex vivo,* establishing a critical role of STING residue 293 in cell death. The *HAQ/SAVI(N153S)* and *AQ/SAVI(N153S)* mice did not have CD4 T cellpenia. The *HAQ/SAVI(N153S), AQ/SAVI(N153S)* mice have more (~10-fold, ~20-fold, respectively) T-regs than *WT/SAVI(N153S)* mice. Remarkably, while they have comparable TBK1, IRF3, and NFκB activation as the *WT/SAVI*, the *AQ/SAVI* mice have no tissue inflammation, regular body weight, and normal lifespan. We propose that STING activation promotes tissue inflammation by depleting T-regs cells *in vivo*. Billions of modern humans have the dominant *HAQ, AQ* alleles. STING research and STING-targeting immunotherapy should consider *TMEM173* heterogeneity in humans.

Teaser

One copy of the common human *HAQ* or *AQ TMEM173* gene prevents the gain-of-function *TMEM173* mutant-caused SAVI disease in mice.

MAIN TEXT

Introduction

STING drives cytosolic DNA-induced type I IFNs production [1]. Recent research revealed that STING promotes inflammation in a variety of inflammatory diseases including nonalcoholic fatty liver disease, nonalcoholic steatohepatitis, kidney injury, neurodegenerative diseases, cardiovascular diseases, obesity, diabetes, and aging [2-9]. The type I IFNs-independent function of STING has also emerged [9-12]. For example, initially described as a type I interferonopathy [13], recent studies in STING-associated vasculopathy with onset in infancy (SAVI) mouse models showed that SAVI is largely independent of type I IFNs [14-17]. In a *STING N153S* mouse model of SAVI, crossing *N153S* mice to IRF3/IRF7, and IFNAR1 knockout mice, N153S mice still developed spontaneous lung diseases [14]. In another example of STING-dependent, type I IFNs-independent inflammatory disease, DNase II-deficient mice developed autoinflammatory arthritis that can be rescued by STING deficiency [18]. But *Dnase II*$^{-/-}$ mice with the STING-S365A mutation still exhibited severe polyarthritis [19,20]. The STING-S365A mutant cannot recruit IRF3 and produce IFNβ [10,11,19,20]. How STING drives inflammation *in vivo,* independent of type I IFNs, remains unknown. The activation of NFκB or NLRP3 inflammasome by STING has been proposed [9,21].

Characterized as an innate immune sensor, STING expression is, paradoxically, high in CD4 T cells [13,22]. Furthermore, STING activation kills mouse and human CD4 T cells *ex vivo* [23-25]. SAVI patients and mouse model had CD4 T cellpenia [13,25]. STING was first discovered as MPYS for its cell growth inhibition and cell death function in mouse B lymphoma cells [26]. STING-mediated cell death is cell type dependent. For example, while STING activation kills human endothelial cells, primary and cancerous T cells, it does not kill mouse MEFs, BMDCs, or BMDMs [27-29]. Second, STING-mediated cell death is type I IFNs-independent [25,27,29]. Multiple cell death pathways, *i.e.,* apoptosis, necroptosis, pyroptosis, ferroptosis, and PANoptosis, are proposed [29-31]. Last, the *in vivo* biological significance of STING-mediated CD4 T cell death is not clear [25,29]. WT and STING$^{-/-}$ mice have similar thymic and pLN CD4^{-}CD8^{-}, CD4^{+}CD8^{+}, and single positive CD4 and CD8 T cell populations [23,24]. The expression of CD4 and CD8 TCR are comparable [23,24]. The naive, memory, or regulatory T cell populations are similar in WT and STING$^{-/-}$ mice that expressed comparable levels of CD69 and CD25 following TCR activation [23,24]. Together, the absence of STING in mice does not alter T cell development or TCR signaling [23]. In humans, SAVI patients with constitutively activated STING have low CD4 T cell numbers [13], and type I IFNs are dispensable for STING-mediated human CD4 T cell death [25]. Notably, SAVI patients (*N154S* or *V155M*) had normal counts of CD8 T and B cells [13].

The human *TMEM173* gene is highly heterogeneous [32,33]. ~50% of people in the U.S. carry at least one copy of non-*WT TMEM173* allele [32]. Among them, the R71H-G230A-R293Q (*HAQ*) is the 2nd most common *TMEM173* allele carried by ~23% of people in the U.S. [32]. However, in East Asians, *WT/HAQ* (34.3%), not *WT/WT* (22.0%), is the most common *TMEM173* genotype [33]. Critically, the *HAQ* allele was positively selected in modern humans outside Africa [34]. Anatomically modern humans outside Africa are descendants of a single Out-of-Africa Migration 50,000~70,000 years ago. ~1.4% of Africans have the *HAQ* allele, while ~63.9% of East Asians are *HAQ* carriers [34]. Haplotype analysis revealed that *HAQ* was derived from G230A-R293Q (*AQ*) allele [34]. Importantly,

the *AQ* allele was negatively selected outside Africa [34]. ~40.1% of Africans are *AQ* carriers, while ~0.4% of East Asians have the *AQ* allele [34]. Importantly, *TMEM173* alleles often have a dominant negative effect likely because the protein STING exists as a homodimer [26,35]. SAVI is an autosomal dominant inflammatory disease [13]. *WT/HAQ* individuals had reduced Pneumovax23®-induced antibody responses compared to *WT/WT* individuals (NCT02471014) [36]. Notably, *AQ* responds to CDNs and produce type I IFNs *in vivo* and *in vitro* [34,37,38], but the *AQ* allele was negatively selected in non-Africans [34]. In contrast, the *HAQ* allele, defective in CDNs-type I IFNs responses [32,33,36,39,40], was positively selected in non-Africans [34] indicating that the CDNs-type I IFNs independent function of STING was essential for the survival of early modern humans outside of Africa.

In this study, we discovered, surprisingly, that the *HAQ*, *AQ* splenocytes are resistant to STING-mediated cell death. We generated *HAQ/SAVI(N153S)* and *AQ/SAVI(N153S)* mice and found that the *HAQ, AQ* alleles prevent CD4 T cellpenia, increase/restore T-regs and alleviate/stop tissue inflammation in SAVI mice, thus providing evidence for the *in vivo* significance of type I IFNs-independent, STING-mediated CD4 T cell death.

Results

STING activation kills mouse spleen CD4, CD8 T and CD19 B cells *ex vivo*.

We first used the synthetic non-CDNs STING agonist diABZI [41] to induce lymphocyte death because diABZI induces cell death without the needs for lipid transfection or detergent for cell permeabilization [28,42] and diABZI is in clinical trials (NCT05514717). Splenocytes from C57BL/6N mice were treated with diABZI in culture, and cell death was determined by Annexin V and Propidium Iodide stain. Splenocyte cell death could be detected as early as 5hrs post diABZI treatment (Figure S1A). Dosage responses showed that ~25ng/ml diABZI could kill 70% of splenocytes (Figure S1B). Similarly, STING agonists DMXAA, and synthetic CDNs RpRpssCDA, killed mouse spleen CD4, CD8 T cells, and CD19 B cells (Figure 1A). Thus, STING activation readily induces mouse lymphocyte death *ex vivo*.

TBK1 activation is required for STING-mediated mouse spleen cell death *ex vivo*.

STING activation can lead to apoptosis, pyroptosis, necroptosis, or ferroptosis [25-31,42,43]. We then treated mouse splenocytes with apoptosis, pyroptosis, necroptosis inhibitors, STING inhibitors H-151, C-176, palmitoylation inhibitor 2-bromopalmitate (2-BP), followed by diABZI stimulation. Inhibitors for NLRP3 (MCC950), RIPK1 (Necrostatin-1), RIPK3 (GSK872), Caspase-1 (VX-795), Caspase-3 (Z-DEVD-FMK), Caspase 1,3,8,9 (Q-VD-Oph), ferroptosis (liproxstatin-1) did not affect diABZI-induced splenocyte cell death *ex vivo* (Figure S1B, S1C). The STING inhibitors H-151, C-176, and 2-BP also could not prevent diABZI-induced cell death (Figure S1C) though they inhibited diABZI-induced IFNβ production (Figure S1D). Instead, the TBK1 inhibitor BX-795 abolished diABZI-induced splenocyte death (Figure S1C).

BX-795 is a multi-kinase inhibitor including 3-phosphoinositide-dependent protein kinase 1 (PDK1) and TBK1 (IC_{50s} = 6 and 11 nM, respectively). However, the treatment of PDK1 inhibitor GSK2334470 (IC50 = 10nM) did not prevent diABZI-induced splenocyte death (Figure 1B). In contrast, GSK8612, a highly potent and selective inhibitor for TBK1, prevented diABZI-induced splenocyte death (Figure 1B). Thus, TBK1 activation is likely critical for STING-mediated lymphocyte cell death *ex vivo*.

HAQ, AQ, Q293 STING knock-in mouse splenocytes are resistant to STING-mediated cell death *ex vivo*.

HAQ and *AQ* are common human *TMEM173* alleles [32-34]. Previously, we reported that *HAQ* knock-in mice are defective in CDNs-induced immune responses, while CDNs responses in *AQ* knock-in mice are similar to WT mice [34]. We treated splenocytes from *HAQ* and *AQ* mice with diABZI *ex vivo* and found, surprisingly, that both *HAQ* and *AQ* splenocytes were resistant to diABZI-induced cell death (Figure 1C, 1D). In comparison, IFNAR1$^{-/-}$ splenocytes were killed by diABZI, confirming that STING-mediated lymphocytes death are type I IFNs-independent (Figure 1C, 1D) [25,27,29].

HAQ and *AQ* share the common A230 and Q293 residues changes. We thus generated a *Q293 TMEM173* knock-in mouse. Notably, the Q293 splenocytes were resistant to STING agonists 2'3'-cGAMP, RpRpssCDA, and diABZI-induced cell death (Figure 1E, 1F). Thus, the residue 293 of STING is critical for its cell death function.

150 ***WT/HAQ*, *WT/AQ* mouse splenocytes are partially resistant to STING-mediated cell**
151 **death *ex vivo*.**
152 *WT/HAQ* (34.3%), not *WT/WT* (22.0%), is the most common human *STING* genotype in
153 East Asians, while *WT/AQ* (28.2%) is the 2nd most common *STING* genotype in Africans
154 [33]. We generated *WT/HAQ*, *WT/AQ* mice and treated the splenocytes with mouse STING
155 agonist DMXAA. *WT/HAQ* and *WT/AQ* splenocytes were protected from 25µg/ml
156 DMXAA-induced cell death (Figure 1G). 100µg/ml DMXAA could kill *WT/HAQ* and
157 *WT/AQ* splenocytes albeit less than *WT/WT* cells (Figure 1G). Thus, the *HAQ* and *AQ*
158 alleles are dominant and likely impact STING activation even in heterozygosity.
159
160 **STING activation kills primary human CD4 T cells, but not CD8 T or CD19 B cells.**
161 STING agonists-based clinical trials in humans have been disappointing (NCT02675439,
162 NCT03010176, NCT05514717) [44,45]. We showed that the human *TMEM173* gene might
163 undergo natural selection during the out-of-Africa migration [34] sensitive to evolutionary
164 pressure. Thus, we investigated STING-mediated death in primary human lymphocytes.
165 Human explant lung cells from the *WT(R232)/WT(R232)* donors were treated with
166 STING agonists 2'3-c GAMP, RpRpssCDA, diABZI for 24hrs in culture. Lymphocyte cell
167 death was determined by Propidium Iodide staining. Different from mouse lymphocytes,
168 diABZI and RpRpssCDA killed human CD4 T but not CD8 T or CD19 B cells (Figure 2A,
169 2B). Human CD8 T and CD19 B cells are resistant to 500ng/ml diABZI-induced cell death
170 (Figure S2A).
171
172 ***WT/HAQ* human CD4 T cells are resistant to low-dose of diABZI-induced cell death.**
173 *WT/HAQ* mouse splenocytes are resistant to low dose diABZI-induced cell death. To
174 extend our observation into primary human T cells, we obtained lung explants from *WT/WT*
175 and *WT/HAQ* individuals (Figure S2B) and treated them with diABZI in culture. 25ng/ml
176 diABZI killed *WT/WT*, but not *WT/HAQ*, human lung CD4 T cells (Figure 2C).
177
178 **diABZI induces cell death in STING-KO human THP-1 cells reconstituted with *WT***
179 **human *STING (R232)* but not *HAQ, AQ or Q293* human *STING* allele.**
180 To further determine cell death influenced by human *TMEM173* alleles *HAQ, AQ* and
181 Q293, we used the *STING-KO* THP-1 cell line because STING agonist induces type I IFNs
182 and cell death in *STING-KO* THP-1 cells expressing WT human STING [31] (Figure S2C,
183 S2D). We, thus, generated stable THP-1 *STING-KO* lines expressing *HAQ, AQ, WT* or
184 *Q293 TMEM173* allele. Cell death was determined by Annexin-V staining. diABZI killed
185 THP-1 *STING-KO* lines expressing *WT* but not *HAQ, AQ,* or *Q293 TMEM173* allele
186 (Figure 2D, 2E). No cell death was induced in the *Q293* THP-1 cells stimulated by 20 to
187 200 ng/ml of diABZI (Figure 2F). diABZI also did not induce STING activation in *Q293*
188 THP-1 cells (Figure 2G). Notably, 50ng/ml diABZI induced p-IRF3 activation and type I
189 IFNs in *AQ* THP-1 cells, but not *HAQ* THP-1 cells (Figure 2H, 2I) indicating that the
190 STING-cell death and STING-IRF3-Type I IFNs pathways can be uncoupled.
191
192 ***HAQ* and *AQ* alleles rescue the lymphopenia and suppress myeloid cell expansion in**
193 ***SAVI(N153S)* mice.**
194 The *in vivo* significance of the STING/MPYS-cell death is unclear. Furthermore, multiple
195 cell death pathways, i.e., apoptosis, necroptosis, pyroptosis, ferroptosis, and PANoptosis,

are proposed [29-31]. The uncertainty likely results from studies using different cell types (primary cells vs cancer cell lines); species (human vs mouse); STING agonists (cGAMP, which requires cell permeabilization by detergents or lipid transfection, vs diABZi, DMXAA that can directly cross the membrane) [23,24,27,28,46]. Critically, which mechanism is relevant *in vivo*, causing T cellpenia is not known. To clarify the *in vivo* significance and mechanisms of STING-mediated cell death, we turned to SAVI mice.

SAVI is an autosomal dominant, inflammatory disease caused by one copy of a gain-of-function STING mutant [13]. CD4 T cellpenia was found in SAVI patients and SAVI mouse models [13,14]. STING activation in SAVI mice is independent of ligands and happens *in vivo*. We thus generated *HAQ/SAVI(N153S)* and *AQ/SAVI(N153S)* mice aiming to establish the *in vivo* significance and mechanism of STING-cell death.

First, *HAQ/SAVI(N153S)* and *AQ/SAVI(N153S)* mice had reduced splenomegaly compared to *WT/SAVI(N153S)* mice though their spleens were still larger than the littermates *WT/HAQ* and *WT/AQ* (Figure 3A, 3B). Next, *HAQ/SAVI(N153S)* and *AQ/SAVI(N153S)* mice had similar spleen B cells and CD4 T cells numbers as the *WT/HAQ*, *WT/AQ* littermates (Figure 2B, 2C). Their $CD8^+$ T cells were lower than their WT littermates but much higher than the *WT/SAVI(N153S)* mice (Figure 3D). Third, spleen myeloid cell numbers, i.e., neutrophils, $Ly6C^{hi}$ monocytes and F4/80 macrophages, were all reduced by half compared to *WT/SAVI(N153S)* mice (Figure 3E~3H). Notably, the *HAQ/SAVI(N153S)* and *AQ/SAVI(N153S)* mice also had restored bone marrow monocyte (Figure S3). Thus, *HAQ* and *AQ* alleles prevent lymphopenia and suppress myeloid cells expansion in *SAVI(N153S)* mice.

The *HAQ* allele alleviates and the *AQ* allele prevents *SAVI(N153S)* disease in mice.

SAVI(N153S) disease is characterized by early onset, failure to thrive (low body weight), persistent lung inflammation, decreased lung function, and young death in humans and mouse models [13,17,46,47]. The *HAQ/SAVI(N153S)* mice weighed more and had an improved lifespan than the *WT/SAVI(N153S)* mice (Figure 4A, 4B). The lifespan, airway resistance and tissue inflammation (lung, liver) were also improved in *HAQ/SAVI(N153S)* mice compared to the *WT/SAVI(N153S)* mice (Figure 4C, 4D, 4J, 4K, S4). However, the pulmonary artery pressure was still elevated in *HAQ/SAVI(N153S)* mice (Figure 4E). Remarkably, the *AQ/SAVI(N153S)* mice had similar body weight and lifespan as the *WT/AQ* mice (Figure 4F, 4G). The airway resistance, pulmonary artery pressure, and tissue inflammation in *AQ/SAVI(N153S)* were similar to the *WT/AQ* littermates (Figure 4H, 4I, 4J, 4K, S4). Thus, the *AQ* allele prevents inflammatory SAVI disease in mice.

diABZI induces similar STING, TBK1, IRF3, NFκB activation in the *AQ/SAVI(N153S)* and *WT/SAVI(N153S)* BMDM.

SAVI was characterized as type I interferonopathy [17]. However, several studies showed that type I IFN signaling and IRF3 activation were dispensable for SAVI disease [14,15,47,48]. *AQ* allele prevents SAVI disease (Figure 4). However, diABZI-treated *AQ/SAVI(N153S)* and *WT/SAVI(N153S)* BMDM had similar TBK1-IRF3 activation and IFNβ production (Figure 5A, 5D). diABZI treatment caused IκBα degradation, and similar TNF production in *WT/SAVI* and *AQ/SAVI* BMDM (Figure 5B, 5E). Furthermore, diABZI activation led to STING protein degradation in *WT/SAVI* and *AQ/SAVI* BMDM (Figure 5C). Last, using cleavable crosslinker dithiobis (succinimidyl propionate (DSP), we showed that STING in

WT/SAVI, AQ/SAVI BMDM forms similar dimer *in situ* (Figure 5F). Thus, the *AQ/SAVI* BMDM had similar STING degradation, TBK1, IRF3, NFκB activation, and dimerization as the *WT/SAVI* BMDM.

The HAQ allele increased, and the _AQ_ allele restored T-regs in _SAVI(N153S)_ mice.

IFNγ was proposed to drive SAVI disease [15,35,48]. We confirmed that *WT/SAVI* CD4 T cells were enriched with IFNγ$^+$ cells (Figure 6A). However, *WT/SAVI* mice have CD4 T cellpenia. Thus, the total numbers of spleen IFNγ$^+$ CD4 T cells were comparable in *WT/SAVI* and *AQ/SAVI* mice (Figure 6A). In contrast, the *HAQ/SAVI mice* had decreased IFNγ$^+$ CD4 T cells (Figure 6A).

The induction of Foxp3 expression in T-reg cells during ongoing autoimmune inflammation resolved inflammation and pathology in mice [49]. CD4 T cellpenia depletes CD4 T-regs. Indeed, *WT/SAVI* mice had ~20-fold reduction of spleen FoxP3$^+$ T-regs compared to *AQ/SAVI* or *WT/WT* littermates (Figure 6B). The *HAQ/SAVI* mice also had ~10-fold more T-regs than the *WT/SAVI* littermate (Figure 6B).

Discussion

This study, using the *HAQ, AQ, SAVI(N153S) TMEM173* knock-in mice, reveals the *in vivo* significance and mechanism of STING-mediated CD4 T cell death. *HAQ, AQ* alleles prevent CD4 T cellpenia, and increase/restore CD4 T-regs in SAVI mice. The results are consistent with previous finding that the impaired CD4 T cell proliferation by the *SAVI(V155M)* mutant could be rescued by the addition of the *HAQ* allele *in vitro* [24]. STING has been increasingly implicated in inflammatory diseases such as nonalcoholic fatty liver disease, nonalcoholic steatohepatitis, cardiomyopathy, obesity, diabetes, neurodegenerative diseases, aging, and kidney injury, many of which are independent of type I IFNs [2,3,9]. It is tempting to suggest that STING activation in CD4 T cells leads to CD4 T-regs depletion that break tissue tolerance and exacerbates tissue inflammation.

Human immunodeficiency virus (HIV) primarily infects CD4 T cells and might activate the STING pathway in CD4 T cells [50-55]. The loss of CD4 T cells is the hallmark of untreated HIV infection [56,57], and the measurement of CD4 T cell count is a central part of HIV care. We found that *HAQ* and *AQ* CD4 T cells are resistant to STING-mediated cell death. Mogensen and colleagues reported that *HAQ/HAQ* was enriched in HIV-infected long-term nonprogressors [39]. These *HAQ/HAQ* individuals had reduced inhibition of CD4 T cell proliferation and a reduced immune response to DNA and HIV [39]. It is likely that HIV infection activates STING-cell death pathway in CD4 T cells. In *HAQ/SAVI* and *AQ/SAVI* mice, one copy of *HAQ*, *AQ* allele suppressed CD4 T cell death. *HAQ*, *AQ* carriers might have fewer HIV-induced CD4 T cell death, thus being long-term nonprogressors in HIV infection-induced Acquired immunodeficiency syndrome (AIDS) [39]. Targeting STING to prevent CD4 T cell death might be a valid therapy for AIDS.

Activating the STING pathway is a promising strategy for cancer immunotherapy [58-64]. Multiple STING agonists are in clinical trials [44,45]. Recently, the safety issue emerged in some STING agonist trials [44,45]. For example, in the STING agonist, ADU-S100, clinical trial, Grade 3/4 treatment-related adverse events were reported in 12.2% of 41 pretreated patients (NCT02675439)[44,45]. The National Institutes of Health defines grade 3 as "incapacitating; unable to perform usual activities; requires absenteeism or bed rest." In a clinical trial using STING antibody-drug-conjugate (ADC) that conjugates diABZI to anti-HER2 Ab, a Grade 5 (fatal) serious adverse event was recorded and deemed related to the STING-ADC (NCT05514717). SAVI disease, driven by overreacting STING, is often fatal. *AQ*, to a less degree, *HAQ*, suppress mortality in SAVI mice. Future STING clinical trials should be based on human *TMEM173* genotype to achieve safe and effective responses.

Mechanistically, apoptosis, pyroptosis, ferroptosis, necroptosis, and PANoptosis have all been reported in STING-mediated cell death [25-31,42,43]. Different cell types and STING agonists used likely contributed to the inconsistency and complexity. Here, we focused on lymphopenia in the SAVI mice that avoids ligand-dependent, non-physiological dosage in STING-mediated cell death. *HAQ* and *AQ* alleles could prevent CD4 T cellpenia in the SAVI mice strongly indicating that residue A230 or Q293 prevent STING-mediated CD4 T cell death *in vivo*. Splenocyte from *Q293* mice were resistant to STING agonists-induced cell death *ex vivo*. Thus, it is likely that the Q293 residue is critical for STING-mediate lymphopenia. Notably, Q293 is outside the C-terminal tail (CTT) (residues 341–379 of human STING) critical for TBK1 recruitment and IRF3 phosphorylation [65] or miniCTT domain (aa343–354) [24], or the UPR motif (aa322–343) [46] important for T cells death *in*

305 *vitro*. Further studies are needed to understand how the aa293 of STING mediates cell
306 death *in vivo*. Noteworthy, *AQ/SAVI* cells had similar TBK1-IRF3, NFκB activation and
307 STING degradation as the *WT/SAVI* cells. Yet, *AQ/SAVI* mice did not have CD4 T
308 cellpenia as *WT/SAVI* mice suggesting that the canonical STING-TBK1-IRF3/NFκB
309 pathway, likely STING oligomerization, is not sufficient for the induction of cell death at
310 the physiological condition.
311 We used the *WT/N153S* knock-in SAVI mouse model that spontaneously develop lung
312 inflammation, T cell cytopenia, and early mortality, mimicking pathological findings in
313 human SAVI patients[16]. Using the *WT/N153S* SAVI mouse model and human Jurkat T cell
314 line, it was proposed that STING activation causes chronic ER stress and unfolded protein
315 response, leading to T cell death by apoptosis [46]. Furthermore, the study showed that
316 crossing *WT/N153S* mice to the OT-I mice reduced ER stress and restored $CD8^+$, but not
317 $CD4^+$, T cells [46]. The restoration of $CD8^+$T cells reduces inflammation and lung disease [46].
318 However, human *WT/N154S* SAVI patients have normal $CD8^+$ T cells numbers [13], and
319 primary human $CD8^+$ T cells are largely resistant to STING-agonists-induced cell death *ex*
320 *vivo* (Figure 2A) [25]. Thus, it is puzzling how restoring $CD8^+$ T cells can rescue SAVI
321 phenotypes since the SAVI patients already have normal $CD8^+$ T cells numbers.
322 Finally, it is unexpected that both *HAQ* and *AQ* alleles are resistant to cell death. Our
323 previous studies showed that the *HAQ* and *AQ* alleles have opposite functions [34]. AQ-
324 STING, not HAQ-STING, responds to CDNs [32-34,36-40,66]. *AQ* mice are lean while *HAQ*
325 mice are fat [34]. Most importantly, *HAQ* was positively selected, while *AQ* was negatively
326 selected, in modern humans outside Africans [34]. Thus, the death pathway of STING is also
327 distinct from the STING function that was naturally selected. Together, we propose that
328 there are at least three unique pathways of STING/MPYS: STING-Type I IFNs, STING-
329 cell death, and STING-fatty acid metabolism.
330 **The limitations of the study**. The poor transferability of mouse to humans is a major issue
331 in STING research [44,45]. The present study used *AQ/SAVI* and *HAQ/SAVI* mice.
332 Confirmation is needed in humans with the identification and evaluation of people who are
333 *AQ/SAVI*, *HAQ/SAVI*.
334

Materials and Methods

Experimental Design. The study was designed to reveal (i) the *in vivo* significance of the type I IFNs-independent, STING-dependent cell death function; (ii) the interplay between common *STING* alleles *HAQ, AQ* and the rare, gain-of-function SAVI STING mutation; (iii). The driver for the inflammatory SAVI disease. Mouse splenocytes, primary human lung cells, human THP-1 cells and *HAQ, AQ, SAVI* knock-in mice were used to establish the *in vivo* significance and human relevance. All the repeats were biological replications that involve the same experimental procedures on different mice. Where possible, treatments were assigned blindly to the experimenter by another individual in the lab. When comparing samples from different groups, samples from each group were analyzed in concert, thereby preventing any biases that might arise from analyzing individual treatments on different days. All experiments were repeated at least twice.

Mice. *WT/SAVI(N153S)* mice were purchased from The Jackson Laboratory. *HAQ*, *AQ* mice were previously generated in the lab [33,34]. The *Q293* mice were generated by Cyagen Biosciences. Briefly, the linearized targeting vector was transfected into JM8A3.N1 C57BL/6N embryonic stem cells. A positive embryonic stem clone was subjected to the generation of chimera mice by injection using C57BL/6J blastocysts as the host. Successful germline transmission was confirmed by PCR sequencing. The heterozygous mice were bred to Actin-flpase mice [The Jackson Laboratory, B6.Cg-Tg (ACTFLPe)9205Dym/J] to remove the neo gene and make the *Q293* knock-in mouse. Age- and gender-matched mice (2 – 6 month old, both male and female) were used for indicated experiments. *WT/SAVI* (male) x *WT/HAQ* (female), *WT/SAVI* (male) x *WT/AQ* (female) breeders were set up to generate *HAQ/SAVI*, *AQ/SAVI* mice. Mice were housed at 22°C under a 12-h light-dark cycle with ad libitum access to water and a chow diet (3.1 kcal/g, Teklad 2018, Envigo, Sommerset, NJ) and bred under pathogen-free conditions in the Animal Research Facility at the University of Florida. Littermates of the same sex were randomly assigned to experimental groups. All mouse experiments were performed by the regulations and approval of the Institutional Animal Care and Use Committee at the University of Florida, IACUC202200000058.

Reagents. Recombinant human IFNβ (R&D, cat no. 8499-IF-010/CF), diABZI (Invivogen, cat no. 2138299-34-8), 2'3'-cGAMP (Invivogen, cat no. tlrl-nacga23-02), DMXAA (Invivogen, cat no. tlrl-dmx), H151 (Invivogen, cat no. inh-h151), RpRpSSCDA (Biolog, cat no. C118), THP1-Dual™ KO-STING Cells (Invivogen, cat no. thpd-kostg). All other chemical inhibitors are from Selleckchem. Mouse TNF alpha ELISA Ready Set Go. (eBioscience, cat no. 88-7324). Mouse IFN-Beta ELISA Kit (PBI, cat no. 42400).

Histology. Lungs and livers were fixed in 10% formalin, paraffin-embedded, and cut into 4-µm sections. Lung, liver sections were then stained for hematoxylin-eosin. All staining procedures were performed by the histology core at the University of Florida. Briefly, tissue sectins were immersed Harris Hematoxylin for 10 seconds, then washed with tap water. Cleard sections were re-immersed in EOSIN stain for ~30 seconds. The sections were washed with tap water until clear, then dehydrate in ascending alcohol solutions (50%,70%,80%,95% x 2, 100% x 2). Afterwards, the sections werer cleared with xylene (3 - 4 x). The sections were mounted on glass slide with permount organic mounting

381 medium for visulization.
382
383 **Lung Function.** Pulmonary function was evaluated using an isolated, buffer-perfused
384 mouse lung apparatus (Hugo Sachs Elektronik, March-Huggstetten, Germany), as
385 previously described [67]. Briefly, mice were anesthetized with ketamine and xylazine and a
386 tracheostomy was performed, and animals were ventilated with room air at 100 breaths/min
387 at a tidal volume of 7 µl/g body weight with a positive end-expiratory pressure of 2 cm
388 H2O using a pressure-controlled ventilator (Hugo Sachs Elektronik, March-Huggstetten,
389 Germany).
390
391 **Isolation of lung cells.** Cells were isolated from the lung as previously described [68]. The
392 lungs were perfused with ice-cold PBS and removed. Lungs were digested in DMEM
393 containing 200µg/ml DNase I (Roche, 10104159001), 25µg/ml Liberase TM (Roche,
394 05401119001) at 37°C for 2 hours. Red blood cells were then lysed and a single cell
395 suspension was prepared by filtering through a 70-µm cell strainer.
396
397 **BMDM activation**
398 BMDMs were induced from mouse bone marrow cells cultured in RPMI 1640 (cat#11965;
399 Invitrogen) with 10% FBS, 2 mM L-glutamine, 1 mM sodium pyruvate, 10 mM HEPES
400 buffer, 1% nonessential amino acids, 50 mM 2-ME, 1% Pen/Strep, with 20ng/ml M-CSF
401 (Kingfisher, RP0407M) for 10 days [33]. STING agonists were added into the culture (no
402 transfection or membrane permeabilization).
403
404 **Flow cytometry.** Single cell suspensions were stained with fluorescent-dye-conjugated
405 antibodies in PBS containing 2% FBS and 1mM EDTA. Surface stains were performed at
406 4°C for 20 min. For intracellular cytokine or transcription factor staining of murine and
407 human cells, cells were fixed and permeabilized with the Foxp3 staining buffer set
408 (eBioscience, cat no 00-5523-00). Cells were washed and stained with surface markers.
409 Cells were then fixed and permeabilized (eBioscience, cat no. 00-5523-00) for intracellular
410 cytokine stain. Data were acquired on a BD LSRFortessa and analyzed using the FlowJo
411 software package (FlowJo, LLC). Cell sorting was performed on the BD FACSAriaIII
412 Flow Cytometer and Cell Sorter. More information on the antibodies used can be found in
413 supplementary table S1.
414
415 **Human lung explants**
416 Human lung explants were procured at the Lung Transplant Center, Division of Pulmonary,
417 Critical Care and Sleep Medicine, Department of Medicine, University of Florida. Donor
418 and patients consent was obtained for a research protocol (UF IRB201902955-Treatment
419 with IFNβ Induces Tolerogenic Lung Dendritic Cells in Human advanced lung disease).
420 Healthy donor lungs were surgically removed postmortem, perfused, small pieces were cut
421 from the right middle and lower lobes for research purpose, and stored in cold Perfadex ®
422 at 4°C for no more than 12 hrs before processing. Ex planted lungs from emphysema lung
423 transplant patients were stored in cold Perfadex ® at 4°C for no more than 12 hrs before
424 the process. No lung explants were procured from prisoners.
425

Statistical Analysis. To gain statistical power, we employ three~four mice/groups to characterize lung immunity. Ten mice/group to monitor animal health. The statistical justification for group size was calculated using the SAS program to calculate the animal numbers. The analysis was carried out using a standard error of 0.5 for immunological assays, and a power of 0.9. All data are expressed as means ± SEM. Statistical significance was evaluated using Prism 9.0 software. Comparisons between two groups were analyzed by performing an unpaired Student's *t* test. Comparisons between more than two groups were analyzed by performing a one-way analysis of variance (ANOVA) with Tukey's multiple comparisons test.

437 **References**

438 1 Barber, G. N. STING: infection, inflammation and cancer. *Nat Rev Immunol* **15**, 760-770
439 (2015).
440 2 Skopelja-Gardner, S., An, J. & Elkon, K. B. Role of the cGAS-STING pathway in
441 systemic and organ-specific diseases. *Nat Rev Nephrol* **18**, 558-572 (2022).
442 3 Bai, J. & Liu, F. cGASSTING signaling and function in metabolism and kidney diseases.
443 *J Mol Cell Biol* **13**, 728-738 (2021).
444 4 Li, H., Guo, X., Aquino, E. & Wu, C. Mini review: STING activation during non-
445 alcoholic fatty liver disease. *Front Nutr* **10**, 1139339 (2023).
446 5 Gulen, M. F., Samson, N., Keller, A., Schwabenland, M., Liu, C., Gluck, S., Thacker, V.
447 V., Favre, L., Mangeat, B., Kroese, L. J., Krimpenfort, P., Prinz, M. & Ablasser, A.
448 cGAS-STING drives ageing-related inflammation and neurodegeneration. *Nature* **620**,
449 374-380 (2023).
450 6 Szego, E. M., Malz, L., Bernhardt, N., Rosen-Wolff, A., Falkenburger, B. H. & Luksch,
451 H. Constitutively active STING causes neuroinflammation and degeneration of
452 dopaminergic neurons in mice. *Elife* **11** (2022).
453 7 Gao, L., Zhang, J., Yang, T., Jiang, L., Liu, X., Wang, S., Wang, X., Huang, Y., Wang,
454 H., Zhang, M., Gong, T., Ma, L., Li, C., He, C., Meng, X. M. & Wu, Y. STING/ACSL4
455 axis-dependent ferroptosis and inflammation promote hypertension-associated chronic
456 kidney disease. *Mol Ther* (2023).
457 8 Yan, M., Li, Y., Luo, Q., Zeng, W., Shao, X., Li, L., Wang, Q., Wang, D., Zhang, Y.,
458 Diao, H., Rong, X., Bai, Y. & Guo, J. Mitochondrial damage and activation of the
459 cytosolic DNA sensor cGAS-STING pathway lead to cardiac pyroptosis and hypertrophy
460 in diabetic cardiomyopathy mice. *Cell Death Discov* **8**, 258 (2022).
461 9 Gao, K. M., Marshak-Rothstein, A. & Fitzgerald, K. A. Type-1 interferon-dependent and
462 -independent mechanisms in cyclic GMP-AMP synthase-stimulator of interferon genes-
463 driven auto-inflammation. *Curr Opin Immunol* **80**, 102280 (2023).
464 10 Yamashiro, L. H., Wilson, S. C., Morrison, H. M., Karalis, V., Chung, J. J., Chen, K. J.,
465 Bateup, H. S., Szpara, M. L., Lee, A. Y., Cox, J. S. & Vance, R. E. Interferon-
466 independent STING signaling promotes resistance to HSV-1 in vivo. *Nat Commun* **11**,
467 3382 (2020).
468 11 Wu, J., Dobbs, N., Yang, K. & Yan, N. Interferon-Independent Activities of Mammalian
469 STING Mediate Antiviral Response and Tumor Immune Evasion. *Immunity* **53**, 115-126
470 e115 (2020).
471 12 Pham, A. T., Oliveira, A. C., Albanna, M., Alvarez-Castanon, J., Dupee, Z., Patel, D., Fu,
472 C., Mukhsinova, L., Nguyen, A., Jin, L. & Bryant, A. J. Non-Interferon-Dependent Role
473 of STING Signaling in Pulmonary Hypertension. *Arterioscler Thromb Vasc Biol* **44**, 124-
474 142 (2024).
475 13 Liu, Y., Jesus, A. A., Marrero, B., Yang, D., Ramsey, S. E., Sanchez, G. A. M.,
476 Tenbrock, K., Wittkowski, H., Jones, O. Y., Kuehn, H. S., Lee, C. R., DiMattia, M. A.,
477 Cowen, E. W., Gonzalez, B., Palmer, I., DiGiovanna, J. J., Biancotto, A., Kim, H., Tsai,
478 W. L., Trier, A. M., Huang, Y., Stone, D. L., Hill, S., Kim, H. J., St Hilaire, C.,
479 Gurprasad, S., Plass, N., Chapelle, D., Horkayne-Szakaly, I., Foell, D., Barysenka, A.,
480 Candotti, F., Holland, S. M., Hughes, J. D., Mehmet, H., Issekutz, A. C., Raffeld, M.,
481 McElwee, J., Fontana, J. R., Minniti, C. P., Moir, S., Kastner, D. L., Gadina, M., Steven,
482 A. C., Wingfield, P. T., Brooks, S. R., Rosenzweig, S. D., Fleisher, T. A., Deng, Z.,

483 Boehm, M., Paller, A. S. & Goldbach-Mansky, R. Activated STING in a vascular and
484 pulmonary syndrome. *N Engl J Med* **371**, 507-518 (2014).
485 14 Luksch, H., Stinson, W. A., Platt, D. J., Qian, W., Kalugotla, G., Miner, C. A., Bennion,
486 B. G., Gerbaulet, A., Rosen-Wolff, A. & Miner, J. J. STING-associated lung disease in
487 mice relies on T cells but not type I interferon. *J Allergy Clin Immunol* **144**, 254-266
488 e258 (2019).
489 15 Stinson, W. A., Miner, C. A., Zhao, F. R., Lundgren, A. J., Poddar, S. & Miner, J. J. The
490 IFN-gamma receptor promotes immune dysregulation and disease in STING gain-of-
491 function mice. *JCI Insight* **7** (2022).
492 16 Warner, J. D., Irizarry-Caro, R. A., Bennion, B. G., Ai, T. L., Smith, A. M., Miner, C. A.,
493 Sakai, T., Gonugunta, V. K., Wu, J., Platt, D. J., Yan, N. & Miner, J. J. STING-
494 associated vasculopathy develops independently of IRF3 in mice. *J Exp Med* **214**, 3279-
495 3292 (2017).
496 17 Fremond, M. L., Hadchouel, A., Berteloot, L., Melki, I., Bresson, V., Barnabei, L.,
497 Jeremiah, N., Belot, A., Bondet, V., Brocq, O., Chan, D., Dagher, R., Dubus, J. C., Duffy,
498 D., Feuillet-Soummer, S., Fusaro, M., Gattorno, M., Insalaco, A., Jeziorski, E.,
499 Kitabayashi, N., Lopez-Corbeto, M., Mazingue, F., Morren, M. A., Rice, G. I., Riviere, J.
500 G., Seabra, L., Sirvente, J., Soler-Palacin, P., Stremler-Le Bel, N., Thouvenin, G.,
501 Thumerelle, C., Van Aerde, E., Volpi, S., Willcocks, S., Wouters, C., Breton, S., Molina,
502 T., Bader-Meunier, B., Moshous, D., Fischer, A., Blanche, S., Rieux-Laucat, F., Crow, Y.
503 J. & Neven, B. Overview of STING-Associated Vasculopathy with Onset in Infancy
504 (SAVI) Among 21 Patients. *J Allergy Clin Immunol Pract* **9**, 803-818 e811 (2021).
505 18 Rodero, M. P., Tesser, A., Bartok, E., Rice, G. I., Della Mina, E., Depp, M., Beitz, B.,
506 Bondet, V., Cagnard, N., Duffy, D., Dussiot, M., Fremond, M. L., Gattorno, M., Guillem,
507 F., Kitabayashi, N., Porcheray, F., Rieux-Laucat, F., Seabra, L., Uggenti, C., Volpi, S.,
508 Zeef, L. A. H., Alyanakian, M. A., Beltrand, J., Bianco, A. M., Boddaert, N., Brouzes, C.,
509 Candon, S., Caorsi, R., Charbit, M., Fabre, M., Faletra, F., Girard, M., Harroche, A.,
510 Hartmann, E., Lasne, D., Marcuzzi, A., Neven, B., Nitschke, P., Pascreau, T., Pastore, S.,
511 Picard, C., Picco, P., Piscianz, E., Polak, M., Quartier, P., Rabant, M., Stocco, G., Taddio,
512 A., Uettwiller, F., Valencic, E., Vozzi, D., Hartmann, G., Barchet, W., Hermine, O.,
513 Bader-Meunier, B., Tommasini, A. & Crow, Y. J. Type I interferon-mediated
514 autoinflammation due to DNase II deficiency. *Nat Commun* **8**, 2176 (2017).
515 19 Li, T., Yum, S., Li, M., Chen, X., Zuo, X. & Chen, Z. J. TBK1 recruitment to STING
516 mediates autoinflammatory arthritis caused by defective DNA clearance. *J Exp Med* **219**
517 (2022).
518 20 Yum, S., Li, M., Fang, Y. & Chen, Z. J. TBK1 recruitment to STING activates both IRF3
519 and NF-kappaB that mediate immune defense against tumors and viral infections. *Proc*
520 *Natl Acad Sci U S A* **118** (2021).
521 21 Gaidt, M. M., Ebert, T. S., Chauhan, D., Ramshorn, K., Pinci, F., Zuber, S., O'Duill, F.,
522 Schmid-Burgk, J. L., Hoss, F., Buhmann, R., Wittmann, G., Latz, E., Subklewe, M. &
523 Hornung, V. The DNA Inflammasome in Human Myeloid Cells Is Initiated by a STING-
524 Cell Death Program Upstream of NLRP3. *Cell* **171**, 1110-1124 e1118 (2017).
525 22 Jin, L., Getahun, A., Knowles, H. M., Mogan, J., Akerlund, L. J., Packard, T. A., Perraud,
526 A. L. & Cambier, J. C. STING/MPYS mediates host defense against Listeria
527 monocytogenes infection by regulating Ly6C(hi) monocyte migration. *J Immunol* **190**,
528 2835-2843 (2013).

23 Larkin, B., Ilyukha, V., Sorokin, M., Buzdin, A., Vannier, E. & Poltorak, A. Cutting Edge: Activation of STING in T Cells Induces Type I IFN Responses and Cell Death. *J Immunol* **199**, 397-402 (2017).

24 Cerboni, S., Jeremiah, N., Gentili, M., Gehrmann, U., Conrad, C., Stolzenberg, M. C., Picard, C., Neven, B., Fischer, A., Amigorena, S., Rieux-Laucat, F. & Manel, N. Intrinsic antiproliferative activity of the innate sensor STING in T lymphocytes. *J Exp Med* **214**, 1769-1785 (2017).

25 Kuhl, N., Linder, A., Philipp, N., Nixdorf, D., Fischer, H., Veth, S., Kuut, G., Xu, T. T., Theurich, S., Carell, T., Subklewe, M. & Hornung, V. STING agonism turns human T cells into interferon-producing cells but impedes their functionality. *EMBO Rep* **24**, e55536 (2023).

26 Jin, L., Waterman, P. M., Jonscher, K. R., Short, C. M., Reisdorph, N. A. & Cambier, J. C. MPYS, a novel membrane tetraspanner, is associated with major histocompatibility complex class II and mediates transduction of apoptotic signals. *Mol Cell Biol* **28**, 5014-5026 (2008).

27 Gulen, M. F., Koch, U., Haag, S. M., Schuler, F., Apetoh, L., Villunger, A., Radtke, F. & Ablasser, A. Signalling strength determines proapoptotic functions of STING. *Nat Commun* **8**, 427 (2017).

28 Kabelitz, D., Zarobkiewicz, M., Heib, M., Serrano, R., Kunz, M., Chitadze, G., Adam, D. & Peters, C. Signal strength of STING activation determines cytokine plasticity and cell death in human monocytes. *Sci Rep* **12**, 17827 (2022).

29 Murthy, A. M. V., Robinson, N. & Kumar, S. Crosstalk between cGAS-STING signaling and cell death. *Cell Death Differ* **27**, 2989-3003 (2020).

30 Li, C., Liu, J., Hou, W., Kang, R. & Tang, D. STING1 Promotes Ferroptosis Through MFN1/2-Dependent Mitochondrial Fusion. *Front Cell Dev Biol* **9**, 698679 (2021).

31 Song, C., Liu, D., Liu, S., Li, D., Horecny, I., Zhang, X., Li, P., Chen, L., Miller, M., Chowdhury, R., Issa, M., Shen, R., Yan, Y., Zhang, F., Zhang, L., Zhang, L., Bai, C., Feng, J., Zhuang, L., Zhang, R., Li, J., Wilkinson, H., Liu, J. & Tao, W. SHR1032, a novel STING agonist, stimulates anti-tumor immunity and directly induces AML apoptosis. *Sci Rep* **12**, 8579 (2022).

32 Jin, L., Xu, L. G., Yang, I. V., Davidson, E. J., Schwartz, D. A., Wurfel, M. M. & Cambier, J. C. Identification and characterization of a loss-of-function human MPYS variant. *Genes Immun* **12**, 263-269 (2011).

33 Patel, S., Blaauboer, S. M., Tucker, H. R., Mansouri, S., Ruiz-Moreno, J. S., Hamann, L., Schumann, R. R., Opitz, B. & Jin, L. The Common R71H-G230A-R293Q Human TMEM173 Is a Null Allele. *J Immunol* **198**, 776-787 (2017).

34 Mansouri, S., Gogoi, H., Patel, S., Katikaneni, D. S., Singh, A., Aybar-Torres, A., de Lartigue, G. & Jin, L. MPYS Modulates Fatty Acid Metabolism and Immune Tolerance at Homeostasis Independent of Type I IFNs. *J Immunol* **209**, 2114-2132 (2022).

35 Patel, S. & Jin, L. TMEM173 variants and potential importance to human biology and disease. *Genes Immun* **20**, 82-89 (2019).

36 Sebastian, M., Hsiao, C. J., Futch, H. S., Eisinger, R. S., Dumeny, L., Patel, S., Gobena, M., Katikaneni, D. S., Cohen, J., Carpenter, A. M., Spiryda, L., Heldermon, C. D., Jin, L. & Brantly, M. L. Obesity and STING1 genotype associate with 23-valent pneumococcal vaccination efficacy. *JCI Insight* **5** (2020).

574 37 Yi, G., Brendel, V. P., Shu, C., Li, P., Palanathan, S. & Cheng Kao, C. Single nucleotide
575 polymorphisms of human STING can affect innate immune response to cyclic
576 dinucleotides. *PLoS One* **8**, e77846 (2013).
577 38 Patel, S., Blaauboer, S. M., Tucker, H. R., Mansouri, S., Ruiz-Moreno, J. S., Hamann, L.,
578 Schumann, R. R., Opitz, B. & Jin, L. Response to Comment on "The Common R71H-
579 G230A-R293Q Human TMEM173 Is a Null Allele". *J Immunol* **198**, 4185-4188 (2017).
580 39 Nissen, S. K., Pedersen, J. G., Helleberg, M., Kjaer, K., Thavachelvam, K., Obel, N.,
581 Tolstrup, M., Jakobsen, M. R. & Mogensen, T. H. Multiple Homozygous Variants in the
582 STING-Encoding TMEM173 Gene in HIV Long-Term Nonprogressors. *J Immunol* **200**,
583 3372-3382 (2018).
584 40 Ruiz-Moreno, J. S., Hamann, L., Shah, J. A., Verbon, A., Mockenhaupt, F. P.,
585 Puzianowska-Kuznicka, M., Naujoks, J., Sander, L. E., Witzenrath, M., Cambier, J. C.,
586 Suttorp, N., Schumann, R. R., Jin, L., Hawn, T. R., Opitz, B. & Group, C. S. The
587 common HAQ STING variant impairs cGAS-dependent antibacterial responses and is
588 associated with susceptibility to Legionnaires' disease in humans. *PLoS Pathog* **14**,
589 e1006829 (2018).
590 41 Ramanjulu, J. M., Pesiridis, G. S., Yang, J., Concha, N., Singhaus, R., Zhang, S. Y.,
591 Tran, J. L., Moore, P., Lehmann, S., Eberl, H. C., Muelbaier, M., Schneck, J. L.,
592 Clemens, J., Adam, M., Mehlmann, J., Romano, J., Morales, A., Kang, J., Leister, L.,
593 Graybill, T. L., Charnley, A. K., Ye, G., Nevins, N., Behnia, K., Wolf, A. I., Kasparcova,
594 V., Nurse, K., Wang, L., Puhl, A. C., Li, Y., Klein, M., Hopson, C. B., Guss, J.,
595 Bantscheff, M., Bergamini, G., Reilly, M. A., Lian, Y., Duffy, K. J., Adams, J., Foley, K.
596 P., Gough, P. J., Marquis, R. W., Smothers, J., Hoos, A. & Bertin, J. Design of
597 amidobenzimidazole STING receptor agonists with systemic activity. *Nature* **564**, 439-
598 443 (2018).
599 42 Messaoud-Nacer, Y., Culerier, E., Rose, S., Maillet, I., Rouxel, N., Briault, S., Ryffel, B.,
600 Quesniaux, V. F. J. & Togbe, D. STING agonist diABZI induces PANoptosis and DNA
601 mediated acute respiratory distress syndrome (ARDS). *Cell Death Dis* **13**, 269 (2022).
602 43 Tang, C. H., Zundell, J. A., Ranatunga, S., Lin, C., Nefedova, Y., Del Valle, J. R. & Hu,
603 C. C. Agonist-Mediated Activation of STING Induces Apoptosis in Malignant B Cells.
604 *Cancer Res* **76**, 2137-2152 (2016).
605 44 Meric-Bernstam, F., Sweis, R. F., Kasper, S., Hamid, O., Bhatia, S., Dummer, R.,
606 Stradella, A., Long, G. V., Spreafico, A., Shimizu, T., Steeghs, N., Luke, J. J.,
607 McWhirter, S. M., Muller, T., Nair, N., Lewis, N., Chen, X., Bean, A., Kattenhorn, L.,
608 Pelletier, M. & Sandhu, S. Combination of the STING Agonist MIW815 (ADU-S100)
609 and PD-1 Inhibitor Spartalizumab in Advanced/Metastatic Solid Tumors or Lymphomas:
610 An Open-Label, Multicenter, Phase Ib Study. *Clin Cancer Res* **29**, 110-121 (2023).
611 45 Meric-Bernstam, F., Sweis, R. F., Hodi, F. S., Messersmith, W. A., Andtbacka, R. H. I.,
612 Ingham, M., Lewis, N., Chen, X., Pelletier, M., Chen, X., Wu, J., McWhirter, S. M.,
613 Muller, T., Nair, N. & Luke, J. J. Phase I Dose-Escalation Trial of MIW815 (ADU-
614 S100), an Intratumoral STING Agonist, in Patients with Advanced/Metastatic Solid
615 Tumors or Lymphomas. *Clin Cancer Res* **28**, 677-688 (2022).
616 46 Wu, J., Chen, Y. J., Dobbs, N., Sakai, T., Liou, J., Miner, J. J. & Yan, N. STING-
617 mediated disruption of calcium homeostasis chronically activates ER stress and primes T
618 cell death. *J Exp Med* **216**, 867-883 (2019).

619 47 Motwani, M., Pawaria, S., Bernier, J., Moses, S., Henry, K., Fang, T., Burkly, L.,
620 Marshak-Rothstein, A. & Fitzgerald, K. A. Hierarchy of clinical manifestations in SAVI
621 N153S and V154M mouse models. *Proc Natl Acad Sci U S A* **116**, 7941-7950 (2019).
622 48 Gao, K. M., Motwani, M., Tedder, T., Marshak-Rothstein, A. & Fitzgerald, K. A.
623 Radioresistant cells initiate lymphocyte-dependent lung inflammation and IFNgamma-
624 dependent mortality in STING gain-of-function mice. *Proc Natl Acad Sci U S A* **119**,
625 e2202327119 (2022).
626 49 Hu, W., Wang, Z. M., Feng, Y., Schizas, M., Hoyos, B. E., van der Veeken, J., Verter, J.
627 G., Bou-Puerto, R. & Rudensky, A. Y. Regulatory T cells function in established
628 systemic inflammation and reverse fatal autoimmunity. *Nat Immunol* **22**, 1163-1174
629 (2021).
630 50 Monroe, K. M., Yang, Z., Johnson, J. R., Geng, X., Doitsh, G., Krogan, N. J. & Greene,
631 W. C. IFI16 DNA sensor is required for death of lymphoid CD4 T cells abortively
632 infected with HIV. *Science* **343**, 428-432 (2014).
633 51 Doitsh, G., Galloway, N. L., Geng, X., Yang, Z., Monroe, K. M., Zepeda, O., Hunt, P.
634 W., Hatano, H., Sowinski, S., Munoz-Arias, I. & Greene, W. C. Cell death by pyroptosis
635 drives CD4 T-cell depletion in HIV-1 infection. *Nature* **505**, 509-514 (2014).
636 52 Jakobsen, M. R., Olagnier, D. & Hiscott, J. Innate immune sensing of HIV-1 infection.
637 *Curr Opin HIV AIDS* **10**, 96-102 (2015).
638 53 Silvin, A. & Manel, N. Innate immune sensing of HIV infection. *Curr Opin Immunol* **32**,
639 54-60 (2015).
640 54 Altfeld, M. & Gale, M., Jr. Innate immunity against HIV-1 infection. *Nat Immunol* **16**,
641 554-562 (2015).
642 55 Krapp, C., Jonsson, K. & Jakobsen, M. R. STING dependent sensing - Does HIV actually
643 care? *Cytokine Growth Factor Rev* **40**, 68-76 (2018).
644 56 Gubser, C., Pitman, M. C. & Lewin, S. R. CD4(+) T cell signatures in HIV infection. *Nat*
645 *Immunol* **20**, 948-950 (2019).
646 57 Morou, A., Brunet-Ratnasingham, E., Dube, M., Charlebois, R., Mercier, E., Darko, S.,
647 Brassard, N., Nganou-Makamdop, K., Arumugam, S., Gendron-Lepage, G., Yang, L.,
648 Niessl, J., Baxter, A. E., Billingsley, J. M., Rajakumar, P. A., Lefebvre, F., Johnson, R.
649 P., Tremblay, C., Routy, J. P., Wyatt, R. T., Finzi, A., Douek, D. C. & Kaufmann, D. E.
650 Altered differentiation is central to HIV-specific CD4(+) T cell dysfunction in
651 progressive disease. *Nat Immunol* **20**, 1059-1070 (2019).
652 58 Hines, J. B., Kacew, A. J. & Sweis, R. F. The Development of STING Agonists and
653 Emerging Results as a Cancer Immunotherapy. *Curr Oncol Rep* **25**, 189-199 (2023).
654 59 Samson, N. & Ablasser, A. The cGAS-STING pathway and cancer. *Nat Cancer* **3**, 1452-
655 1463 (2022).
656 60 Liu, Y., Lu, X., Qin, N., Qiao, Y., Xing, S., Liu, W., Feng, F., Liu, Z. & Sun, H. STING,
657 a promising target for small molecular immune modulator: A review. *Eur J Med Chem*
658 **211**, 113113 (2021).
659 61 Zheng, J., Mo, J., Zhu, T., Zhuo, W., Yi, Y., Hu, S., Yin, J., Zhang, W., Zhou, H. & Liu,
660 Z. Comprehensive elaboration of the cGAS-STING signaling axis in cancer development
661 and immunotherapy. *Mol Cancer* **19**, 133 (2020).
662 62 Corrales, L., Glickman, L. H., McWhirter, S. M., Kanne, D. B., Sivick, K. E., Katibah, G.
663 E., Woo, S. R., Lemmens, E., Banda, T., Leong, J. J., Metchette, K., Dubensky, T. W., Jr.

& Gajewski, T. F. Direct Activation of STING in the Tumor Microenvironment Leads to Potent and Systemic Tumor Regression and Immunity. *Cell Rep* **11**, 1018-1030 (2015).

63 Fu, J., Kanne, D. B., Leong, M., Glickman, L. H., McWhirter, S. M., Lemmens, E., Mechette, K., Leong, J. J., Lauer, P., Liu, W., Sivick, K. E., Zeng, Q., Soares, K. C., Zheng, L., Portnoy, D. A., Woodward, J. J., Pardoll, D. M., Dubensky, T. W., Jr. & Kim, Y. STING agonist formulated cancer vaccines can cure established tumors resistant to PD-1 blockade. *Sci Transl Med* **7**, 283ra252 (2015).

64 Barber, G. N. Innate immune DNA sensing pathways: STING, AIMII and the regulation of interferon production and inflammatory responses. *Curr Opin Immunol* **23**, 10-20 (2011).

65 Liu, S., Cai, X., Wu, J., Cong, Q., Chen, X., Li, T., Du, F., Ren, J., Wu, Y. T., Grishin, N. V. & Chen, Z. J. Phosphorylation of innate immune adaptor proteins MAVS, STING, and TRIF induces IRF3 activation. *Science* **347**, aaa2630 (2015).

66 Movert, E., Bolarin, J. S., Valfridsson, C., Velarde, J., Skrede, S., Nekludov, M., Hyldegaard, O., Arnell, P., Svensson, M., Norrby-Teglund, A., Cho, K. H., Elhaik, E., Wessels, M. R., Raberg, L. & Carlsson, F. Interplay between human STING genotype and bacterial NADase activity regulates inter-individual disease variability. *Nat Commun* **14**, 4008 (2023).

67 Cai, J., Gehrau, R., Tu, Z., Leroy, V., Su, G., Shang, J., Mas, V. R., Emtiazjoo, A., Pelaez, A., Atkinson, C., Machuca, T., Upchurch, G. R., Jr. & Sharma, A. K. MicroRNA-206 antagomiRenriched extracellular vesicles attenuate lung ischemiareperfusion injury through CXCL1 regulation in alveolar epithelial cells. *J Heart Lung Transplant* **39**, 1476-1490 (2020).

68 Mansouri, S., Katikaneni, D. S., Gogoi, H., Pipkin, M., Machuca, T. N., Emtiazjoo, A. M. & Jin, L. Lung IFNAR1(hi) TNFR2(+) cDC2 promotes lung regulatory T cells induction and maintains lung mucosal tolerance at steady state. *Mucosal Immunol* **13**, 595-608 (2020).

Acknowledgments

Funding: National Institutes of Health grant HL152163 (L.J.).

Author contributions:

Conceptualization: LJ
Methodology: AAT, LAS, ATP, AME
Investigation: AAT, LAS, ATP, AKS, AJB, LJ
Supervision: LJ
Writing—original draft: LJ
Writing—review & editing: LJ, AJB, AKS

Competing interests: Authors declare that they have no competing interests.

Data and materials availability: All data are available in the main text or the supplementary materials.

Figure and Captions

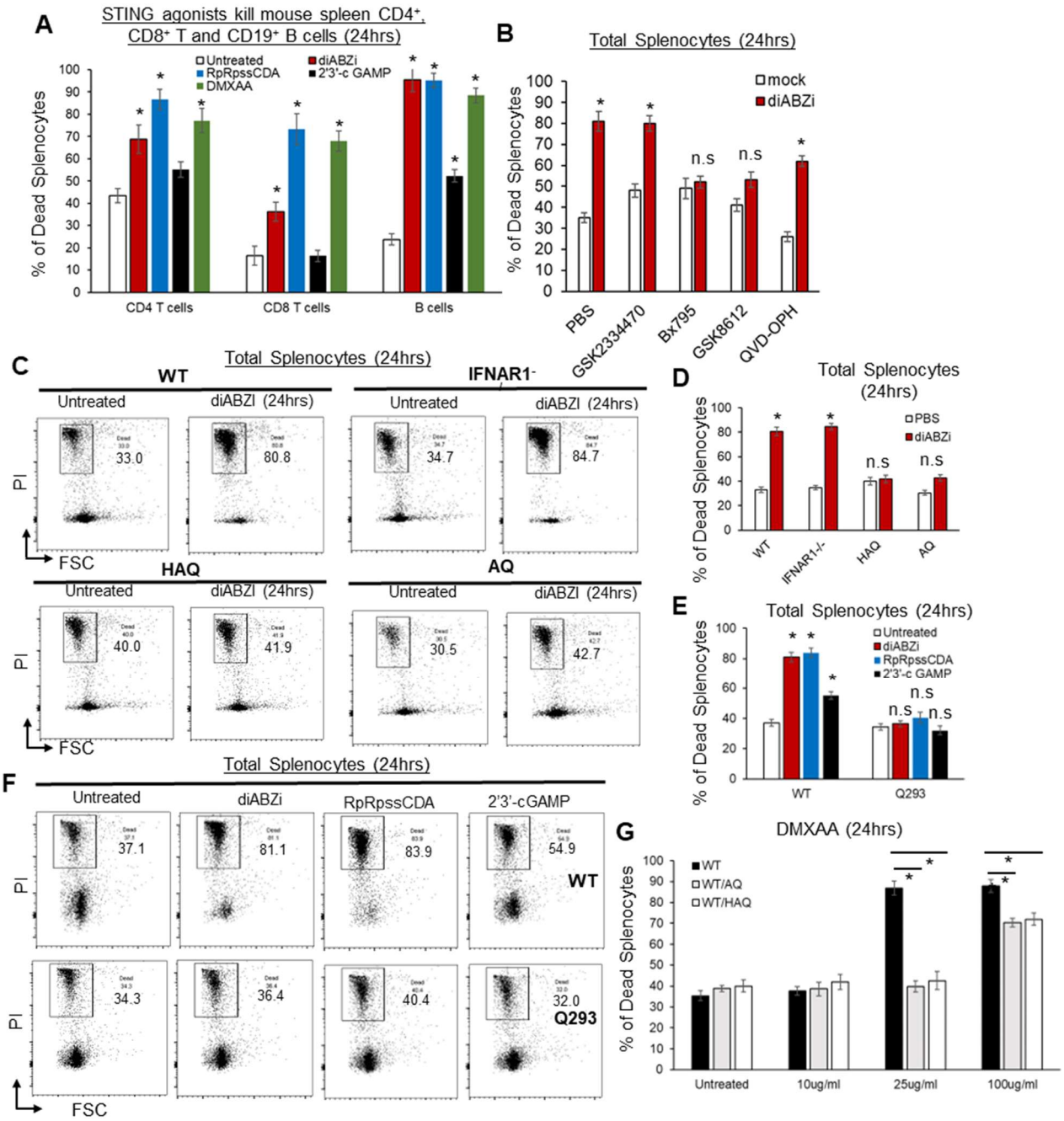

Fig. 1. Splenocytes from *HAQ, AQ*, and *Q293* mice are resistant to STING-mediated cell death *ex vivo*. (A). C57BL/6N splenocytes were treated directly (no transfection) with diABZI (100ng/ml), RpRpssCDA (5 µg/ml) or 2′3′-cGAMP (10µg/ml), DMXAA (25µg/ml) for 24hrs in culture. CD4, CD8 T cells and CD19 B cells death were determined by PI staining. (**B**). Splenocytes from C57BL/6N mice were pre-treated with indicated small molecules, GSK2334470 (1.25µM), GSK8612 (2.5µM), Bx-795 (0.5µM), QVD-OPH (25µM) for 2hrs. diABZI

721 (100ng/ml) was added in culture for another 24hrs. Dead cells were determined by
722 PI staining. (**C-D).** Flowcytometry of *HAQ*, *AQ*, IFNAR1$^{-/-}$ or C57BL/6N
723 splenocytes treated with diABZI (100ng/ml) for 24hrs. Cell death was determined
724 by PI staining. (**E-F)**. *Q293* or the *WT* littermates splenocytes were treated with
725 diABZI (100ng/ml), RpRpssCDA (5 µg/ml) or 2′3′-cGAMP 10µg/ml) for 24h. Cell
726 death was determined by PI staining. (**G).** *WT/HAQ*, *WT/AQ*, or *WT/WT* littermates
727 splenocytes were treated with DMXAA (10, 25 or 100µg/ml) for 24h. Cell death
728 was determined by PI staining. Data are representative of three independent
729 experiments. Graphs represent the mean with error bars indication s.e.m. *p* values
730 are determined by one-way ANOVA Tukey's multiple comparison test (**A, E, G**)
731 or unpaired student T-test (**B, D**). * $p<0.05$. n.s: not significant.
732
733

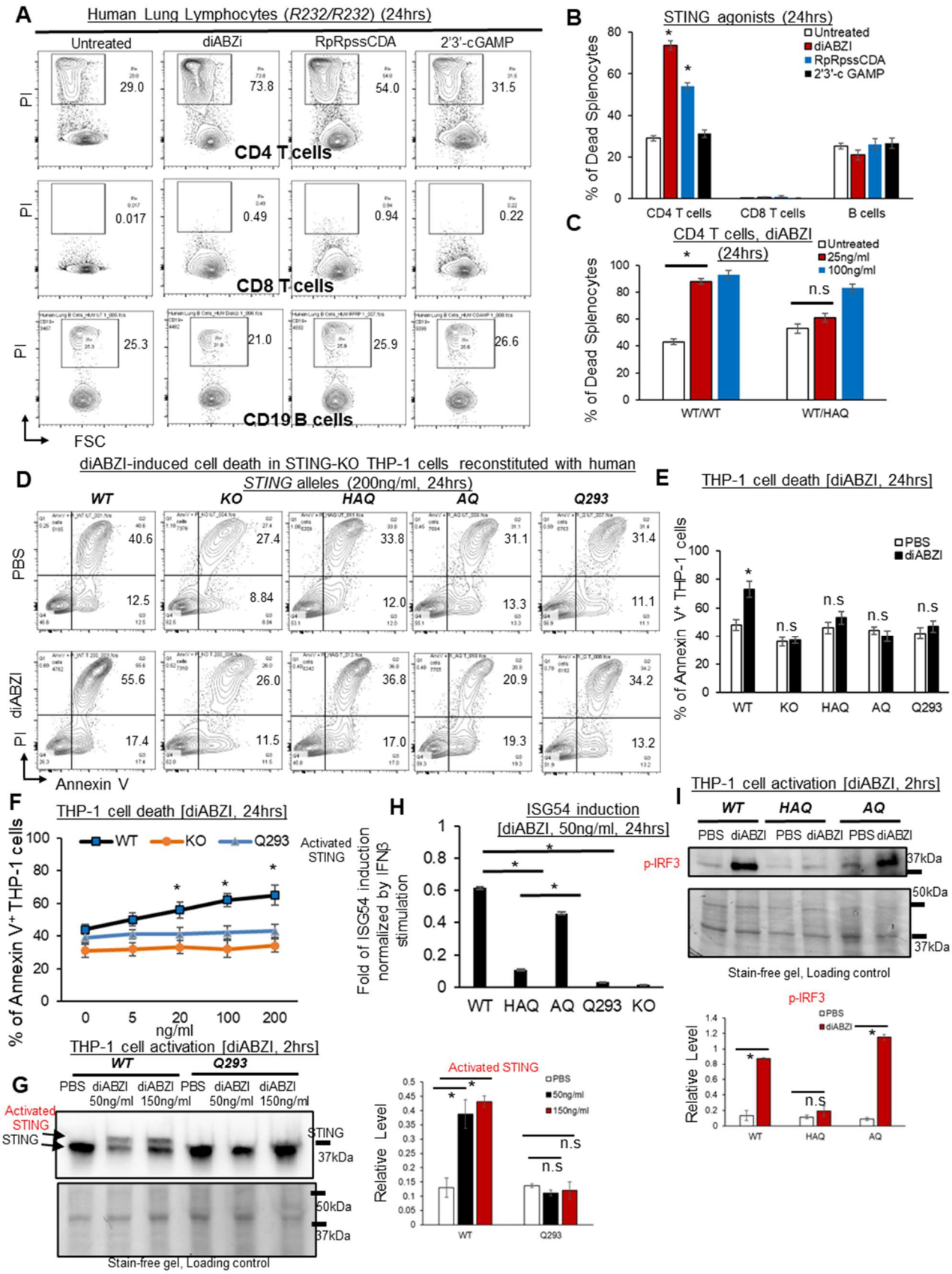
A
Human Lung Lymphocytes (R232/R232) (24hrs)
Untreated
diABZi
RpRpssCDA
2'3'-cGAMP
PI
29.0
73.8
54.0
31.5
CD4 T cells
0.017
0.49
0.94
0.22
CD8 T cells
25.3
21.0
25.9
26.6
CD19 B cells
FSC
B
STING agonists (24hrs)
% of Dead Splenocytes
Untreated
diABZI
RpRpssCDA
2'3'-c GAMP
CD4 T cells
CD8 T cells
B cells
C
CD4 T cells, diABZI (24hrs)
Untreated
25ng/ml
100ng/ml
n.s
WT/WT
WT/HAQ
D
diABZI-induced cell death in STING-KO THP-1 cells reconstituted with human STING alleles (200ng/ml, 24hrs)
WT
KO
HAQ
AQ
Q293
PBS
diABZI
40.6
12.5
27.4
8.84
33.8
12.0
31.1
13.3
31.4
11.1
55.6
17.4
26.0
11.5
36.8
17.0
20.9
19.3
34.2
13.2
Annexin V
E
THP-1 cell death [diABZI, 24hrs]
% of Annexin V+ THP-1 cells
PBS
diABZI
n.s
WT
KO
HAQ
AQ
Q293
F
THP-1 cell death [diABZI, 24hrs]
WT
KO
Q293
Activated STING
% of Annexin V+ THP-1 cells
ng/ml
H
ISG54 induction [diABZI, 50ng/ml, 24hrs]
Fold of ISG54 induction normalized by IFNβ stimulation
WT
HAQ
AQ
Q293
KO
I
THP-1 cell activation [diABZI, 2hrs]
WT
HAQ
AQ
PBS
diABZI
p-IRF3
37kDa
50kDa
Stain-free gel, Loading control
Relative Level
G
THP-1 cell activation [diABZI, 2hrs]
WT
Q293
PBS
diABZI 50ng/ml
diABZI 150ng/ml
Activated STING
STING
37kDa
50kDa
Stain-free gel, Loading control
50ng/ml
150ng/ml
n.s

735 **Fig. 2. *HAQ* , *AQ*, and *Q293* human cells are resistant to STING agonists-induced**
736 **death. (A-B).** Total human Lung cells from *WT/WT* individuals were treated with
737 diABZi (100ng/ml) for 24hrs. Cell death in CD4, CD8 T cells and CD19 B cells
738 were determined by PI staining. (**C**). Total lung cells from a *WT/HAQ* (2
739 individuals) and a *WT/WT* (3 individuals) were treated with diABZi (25, 100ng/ml)
740 for 24h. Cell death in CD4 T cells was determined by PI staining. (**D-E**). STING-
741 KO THP-1 cells (Invivogen,, cat no. thpd-kostg) were stably reconstituted with
742 human *WT (R232), HAQ*, *AQ*, *Q293*. Cells were treated with diABZI (200ng/ml)
743 in culture for 24 hrs. Dead cells were determined by Annexin V staining. (**F).**
744 STING-KO THP-1 cells stably reconstituted with human *WT (R232), Q293* were
745 treated with indicated dose of diABZI for 24hs in culture. Dead cells were
746 determined by Annexin V staining. (**G**). STING-KO THP-1 cells stably
747 reconstituted with human *WT (R232), Q293* were treated with indicated dose of
748 diABZI for 2hs in culture. STING activation was detected by anti-STING antibody
749 (Proteintech, #19851-1-AP). (**H**). STING-KO THP-1 cells stably reconstituted with
750 human *WT (R232), HAQ*, *AQ*, *Q293* were treated with 50ng/ml diABZI in culture
751 for 24hrs. ISG-54 reporter luciferase activity was determined in cell supernatant
752 and normalized to 10ng/ml IFNβ-stimulated ISG-54 luciferase activity. (**I).**
753 STING-KO THP-1 cells stably reconstituted with human *WT (R232), HAQ*, *AQ*
754 were treated with 50ng/ml diABZI in culture for 2hrs. STING and IRF3 activation
755 were determined by anti-STING antibody and anti-p IRF3 antibody (CST, Ser396,
756 clone 4D4G). Densitometry was determined by ImageLab 5. Data are
757 representative of three independent experiments. Graphs represent the mean with
758 error bars indication s.e.m. *p* values determined by one-way ANOVA Tukey's
759 multiple comparison test (**B, C, F, H, G**) or unpaired student T-test (**E, I**). * $p<0.05$,
760 n.s: not significant.
761
762

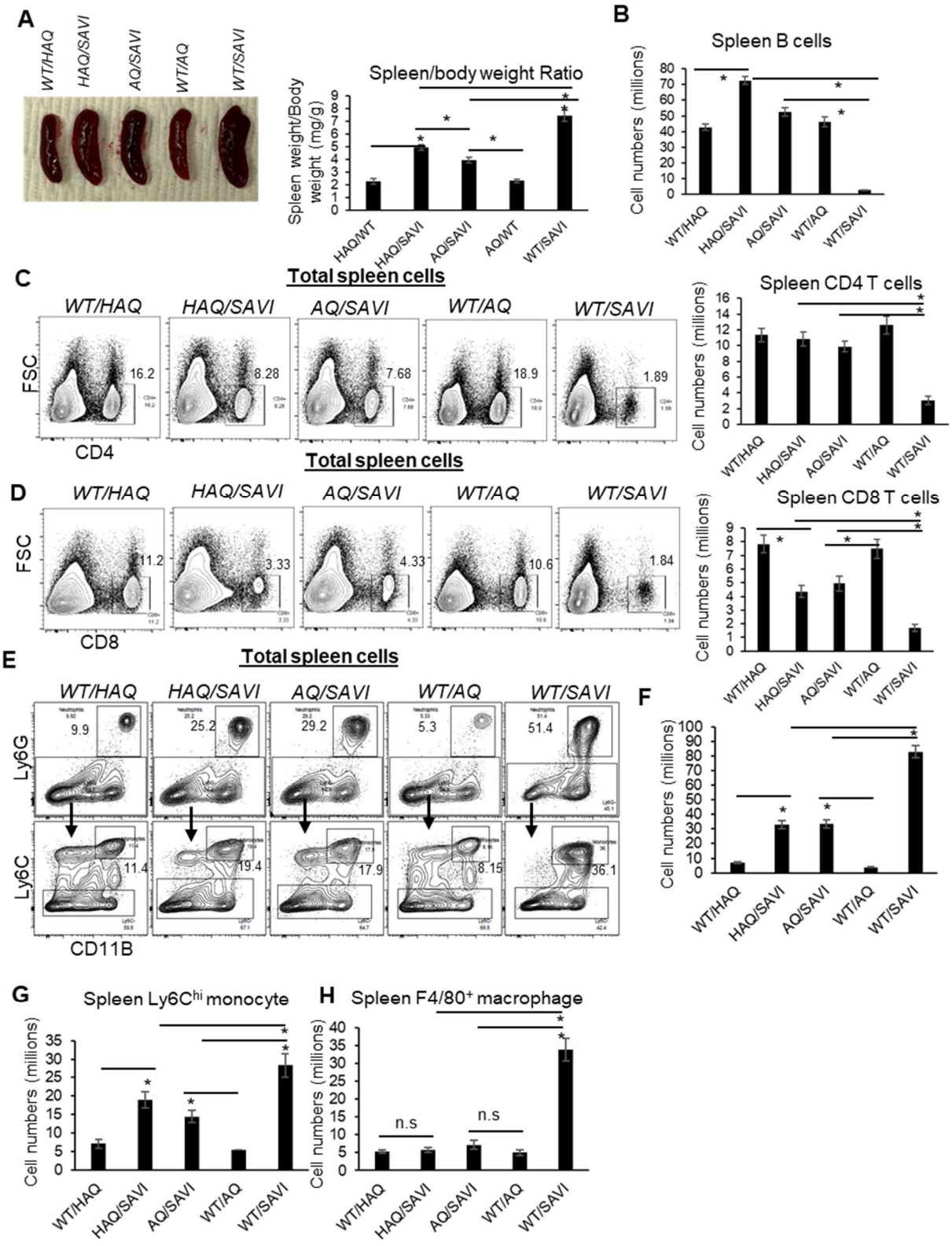

Fig. 3. *HAQ* and *AQ* rescue the lymphopenia and suppress myeloid cell expansion in *SAVI (N153S)* mice. (A). The size and weight of spleens from *WT/HAQ,*

767 *HAQ/SAVI, AQ/SAVI, WT/AQ, WT/SAVI*. **(B-D).** Spleen $CD19^+$ B cells, CD4, CD8
768 T cells were determined in the indicated mice by Flow. (**E-H).** Spleen $Ly6G^+$
769 neutrophils, $Ly6C^{hi}$ monocytes and $F4/80^+$ macrophage was determined in the
770 indicated mice by Flow. Data are representative of three independent experiments.
771 n=3~5 mice/group. Graphs represent the mean with error bars indication s.e.m. *P*
772 values are determined by one-way ANOVA Tukey's multiple comparison test. *****
773 $p<0.05$, n.s: not significant.
774

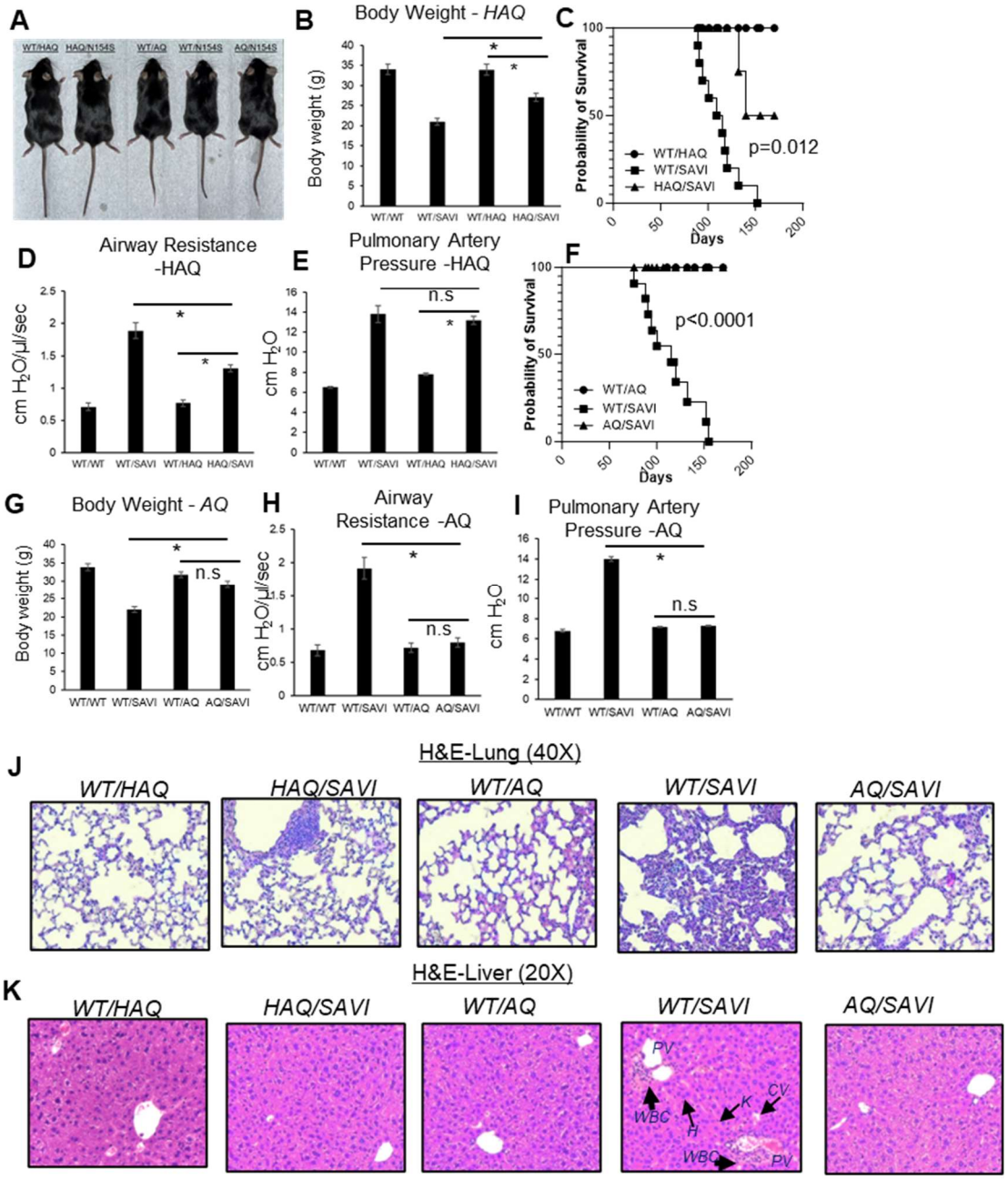

Fig. 4. *HAQ* and *AQ* alleles prevent *SAVI(N153S)* disease in mice. (A, B, G). The size and body weight of *HAQ/SAVI*, *AQ/SAVI*, *WT/SAVI* and their littermates *WT/HAQ*, *WT/AQ* mice. (**D, E, H, I**). Airway resistance, and pulmonary artery pressure were determined as described in **Materials and Methods**. **(C, F).** *HAQ/SAVI, AQ/SAVI, WT/SAVI* (10 mice/group), were monitored for survival by Kaplan-Meier. (**J, K**). Representative hematoxylin and eosin (H&E) staining of lung, liver sections from indicated mice. n=3~5 mice/group. Data are representative of 3 independent experiments. Graphs represent the mean with error bars indication s.e.m. *p* values are determined by one-way ANOVA Tukey's multiple comparison test. * $p<0.05$,

787 **$p<0.01$. n.s.: not significant. **WBC**: white blood cells; **H**: hepatocytes; **K**: Kupper
788 cells; **PV**: portal vein; **CV**: central vein.
789
790
791

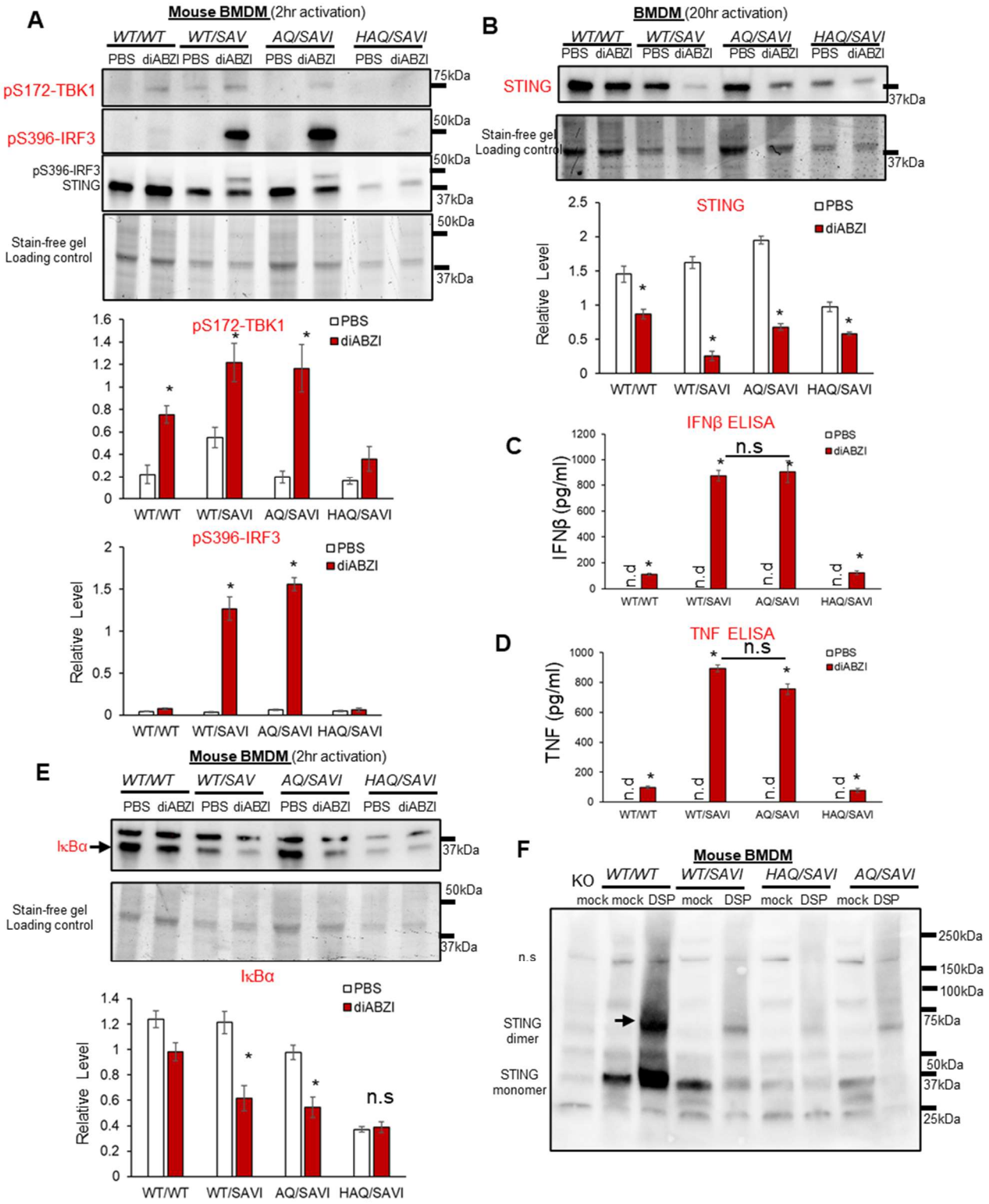

Fig. 5. ***AQ/SAVI(N153S)*** **cells had similar TBK1-IRF3, NFκB activation and STING degradation as the** ***WT/SAVI(N153S)*** **cells.** (**A, B).** BMDM from *WT/WT, WT/SAVI, HAQ/SAVI* and *AQ/SAVI* were treated with 100ng/ml diABZi in culture

797 for 2 hrs. Cells were lysed and run on a 4~20% Mini-PROTEAN TGX Stain-Free
798 Precast Gel. The blot was probed for phospho-Thr172-TBK1 antibody (CST, clone
799 D52C2), phosphor-Ser 396-IRF3 (CST, clone 4D4G), STING (Proteintech,
800 #19851-1-AP) and IκBα (CST, clone 44D4) antibody. **(C).** BMDM from *WT/WT,*
801 *WT/SAVI, HAQ/SAVI* and *AQ/SAVI* were treated with 100ng/ml diABZi in culture
802 for 24 hrs. Cells were lysed and run on a 4~20% Mini-PROTEAN TGX Stain-Free
803 Precast Gel. The blot was probed for STING antibody (Proteintech, 19851-1-AP).
804 (**D, E**). IFNβ and TNF were determined by ELISA in the cell supernatant from **C**.
805 (**F).** BMDM from *WT/WT, WT/SAVI, HAQ/SAVI* and *AQ/SAVI* were treated with
806 400μM cleavable chemical crosslinker DSP (Pierce™, cat no: PG82081) in PBS
807 for 1 hr at 4°C. Cells were washed with PBS and lysed in RIPA buffer. Whole cell
808 lysate was mixed with 4x Laemmli Sample Buffer (BioRad, cat no 1610747)
809 containing 5% 2-mercaptoethanol, heated at 95°C for 10 min and, run on a 4~20%
810 Mini-PROTEAN TGX Stain-Free Precast Gel. The blot was probed for STING
811 antibody (Proteintech, 19851-1-AP). Densitometry was determined by ImageLab
812 5. Data are representative of three independent experiments. Graphs represent the
813 mean with error bars indication s.e.m. *p* values are determined by unpaired student
814 T-test (**A-E**) or one-way ANOVA Tukey's multiple comparison test (**D, E**). *
815 $p<0.05$, ** $p<0.01$, *** $p<0.001$. n.s.: not significant; n.d: not detected.
816
817

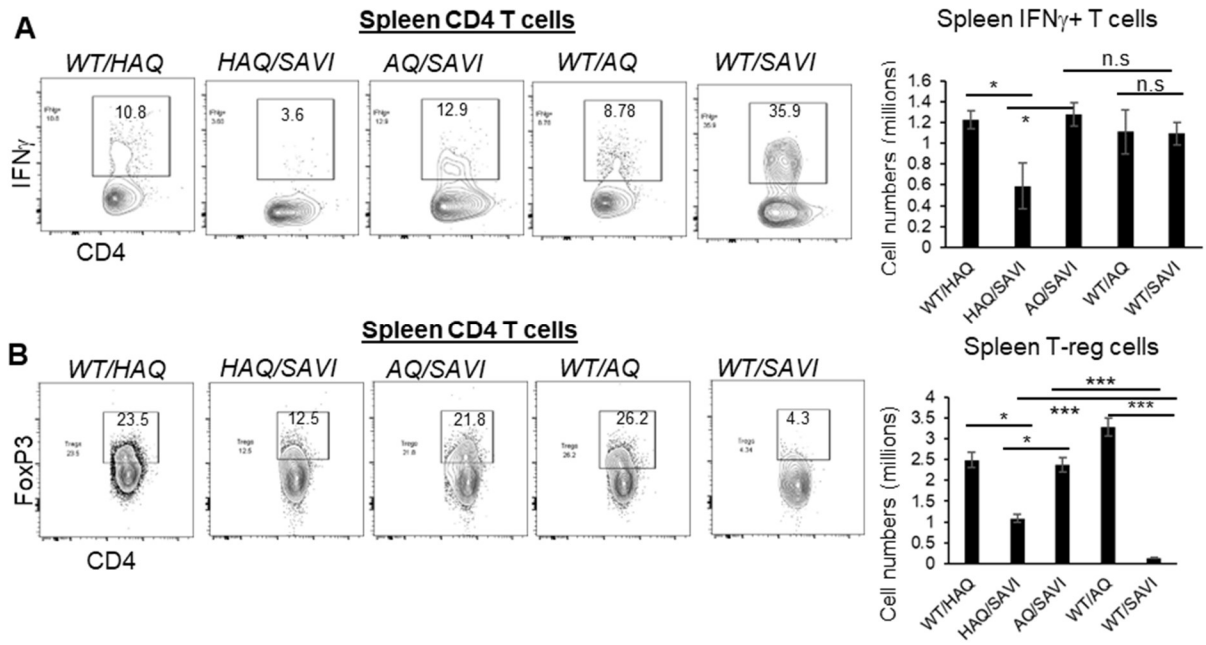

Fig. 6. *HAQ/SAVI(N153S)* and *AQ/SAVI(N153S)* cells had 10-fold and 20-fold increased spleen T-regs compared to *WT/SAVI* mice. (A). Flow cytometry analysis of IFNγ producing spleen $CD4^+$ T cells from *WT/HAQ, WT/AQ, WT/SAVI, HAQ/SAVI* and *AQ/SAVI* mice. (**B**). Flow cytometry analysis of $CD4^+$ $FoxP3^+$ spleen T-regs. n=3~5 mice/group. Data are representative of 3 independent experiments. Graphs represent the mean with error bars indication s.e.m. *p* values are determined by one-way ANOVA Tukey's multiple comparison test. * $p<0.05$, ** $p<0.01$, *** $p<0.001$. n.s.: not significant.

Supplementary Materials for

The common *TMEM173 HAQ, AQ* alleles rescue CD4 T cellpenia, restore T-regs, and prevent SAVI (N153S) inflammatory disease in mice.

Alexandra Aybar-Torres *et al.*

*Corresponding author. Email: lei.jin@medicine.ufl.edu

This PDF file includes:

Figs. S1 to S4

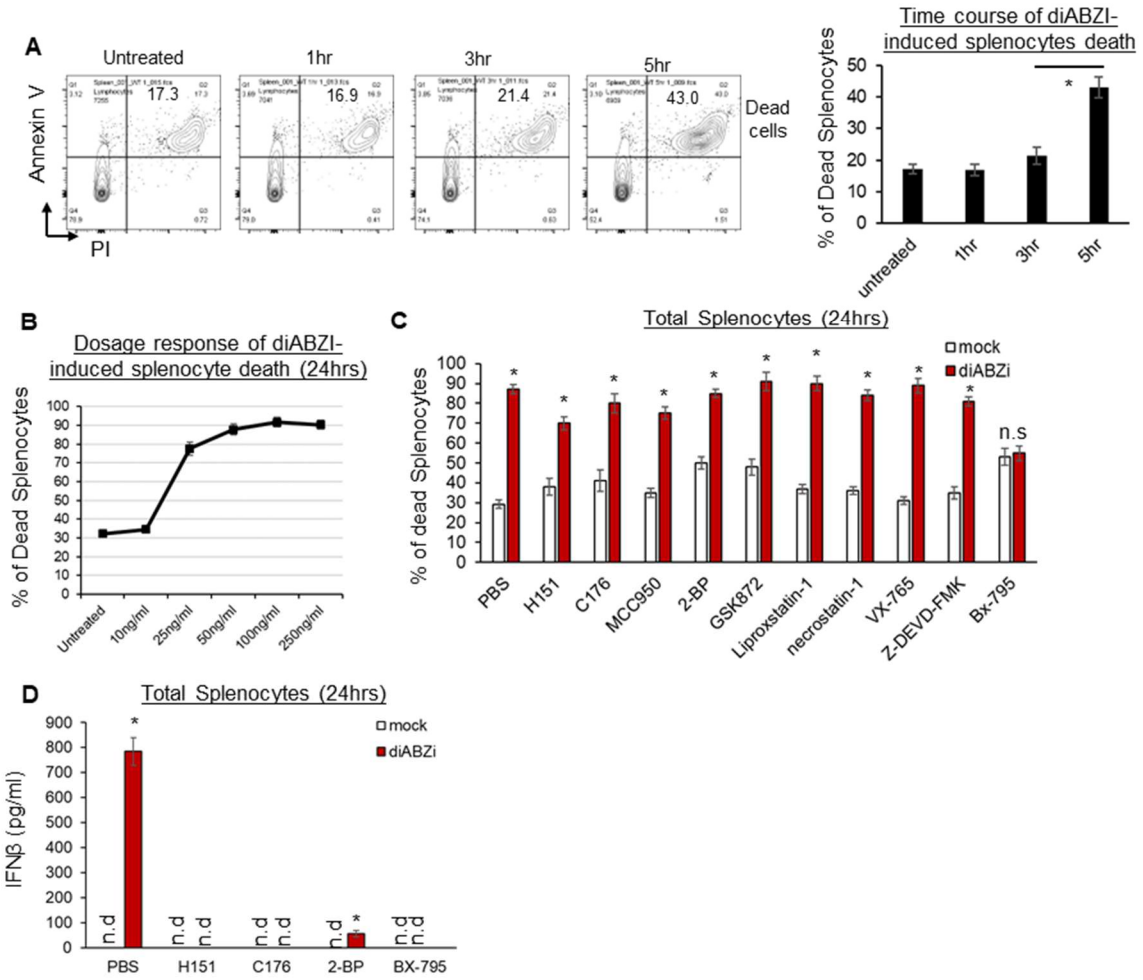

Fig. S1.

Bx-795 inhibits diABZI-induced mouse splenocyte death. (A). Splenocytes from C57BL/6N mice were treated with 100ng/ml diABZI in culture for the indicated time. Dead cells were determined by PI and Annexin V staining. (**B).** Splenocytes from C57BL/6N mice were treated with indicated dose of diABZi in culture for 24hrs. Dead cells were determined by PI staining. **(C)**. Splenocytes from C57BL/6N mice were pre-treated with indicated small molecules, H151 (10μg/ml), C176 (1μM), MCC950 (1.25μM), 2-BP (20μM), GSK872 (312.5nM), Liproxstatin-1 (1μM), necrostatin-1 (10μM), VX-765 (1μM), Z-DEVD-FMK (25μM), Bx-795 (0.5μM) for 2hrs. diABZi (100ng/ml) was added in culture for another 24hrs. Dead cells were determined by PI staining. (**D**). IFNβ was determined in the cell supernatant from **C** by ELISA. Data are representative of three independent experiments. Graphs represent the mean with error bars indication s.e.m. n=3~5 mice/group. *p* values are determined by one-way ANOVA Tukey's multiple comparison test (**A, D**) or unpaired student T-test (**C**). * $p<0.05$. n.s: not significant. n.d: not detected.

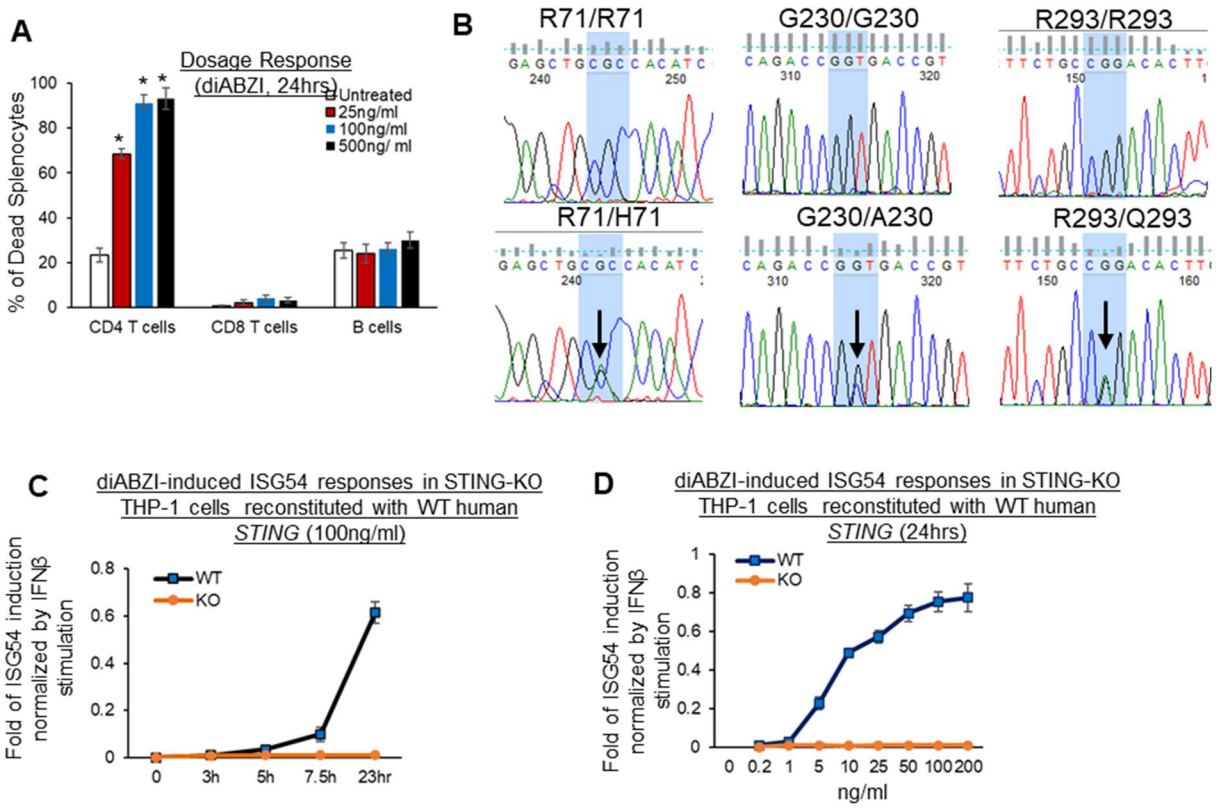

Fig. S2.

STING activation in primary human cells and THP-1 cells reconstituted with *WT* human *STING*. (A). Total human Lung cells from *WT/WT* individuals were treated with indicated dose of diABZi for 24hrs. Cell death in CD4, CD8 T cells and CD19 B cells were determined by PI staining. **(B).** Sequencing results of human *TMEM173* gene in *WT/WT* and *WT/HAQ* individuals. **(C-D)**. STING-KO THP-1 cells stably reconstituted with human *WT (R232)* were treated with indicated dose of diABZI for indicated time in culture. ISG-54 reporter luciferase activity was determined in cell supernatant and normalized to 10ng/ml IFNβ-stimulated ISG-54 luciferase activity. Data are representative of at least two independent experiments. Graphs represent the mean with error bars indication s.e.m. *p* values determined by one-way ANOVA Tukey's multiple comparison test. * $p<0.05$, n.s: not significant**.**

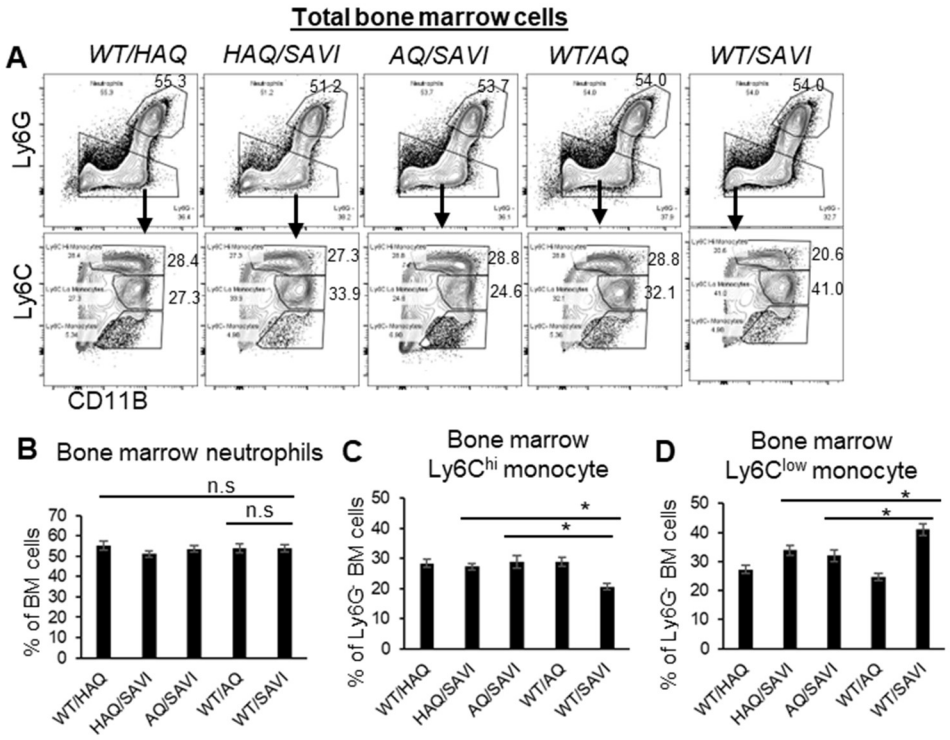

Fig. S3.

***HAQ* and *AQ* restore bone marrow monocytes in *SAVI (N153S)* mice.** (**A-D).** Flow analysis of $Ly6G^{+}CD11B^{+}$ neutrophils and $Ly6G^{-}Ly6C^{+}CD11B^{+}$ bone marrow monocytes from HAQ/SAVI, AQ/SAVI, WT/SAVI and their littermates. n=3~5 mice/group. Data are representative of three independent experiments. Graphs represent the mean with error bars indication s.e.m. *P* values are determined by one-way ANOVA Tukey's multiple comparison test. * $p<0.05$, n.s: not significant.

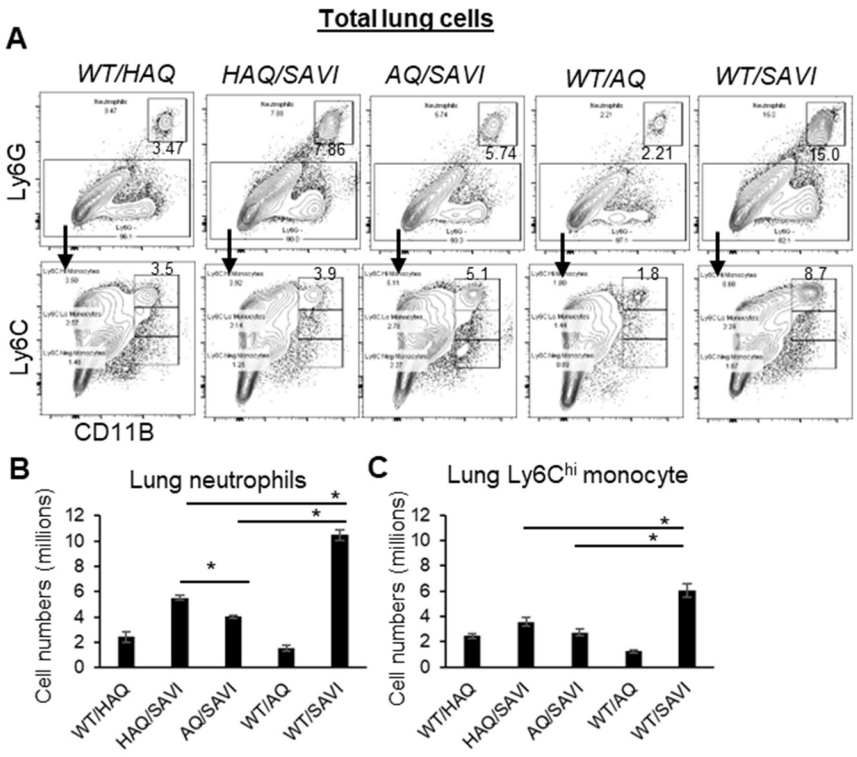

Fig. S4.

***HAQ, AQ* suppress lung myeloid cells infiltration in *SAVI(N153S)* mice**. **(A-C).** Flow analysis of lung $Ly6G^{+}CD11B^{+}$ neutrophils and $Ly6G^{-}Ly6C^{+}CD11B^{+}$ monocytes from *HAQ/SAVI, AQ/SAVI, WT/SAVI and their littermates WT/HAQ, WT/AQ* mice. n=3~5 mice/group. Data are representative of three independent experiments. Graphs represent the mean with error bars indication s.e.m. *P* values are determined by one-way ANOVA Tukey's multiple comparison test. * $p<0.05$.